

See discussions, stats, and author profiles for this publication at: <https://www.researchgate.net/publication/235683549>

Novel Synthetic Strategy for the Sulfonation of Polybutadiene and Styrene–Butadiene Copolymers

ARTICLE *in* MACROMOLECULES · FEBRUARY 2013

Impact Factor: 5.8 · DOI: 10.1021/ma301972m

CITATIONS

9

READS

65

3 AUTHORS, INCLUDING:



[Antonio Buonerba](#)

Università degli Studi di Salerno

42 PUBLICATIONS 85 CITATIONS

[SEE PROFILE](#)



[V. Speranza](#)

Università degli Studi di Salerno

48 PUBLICATIONS 385 CITATIONS

[SEE PROFILE](#)

Novel Synthetic Strategy for the Sulfonation of Polybutadiene and Styrene–Butadiene Copolymers

Antonio Buonerba,^{†,‡} Vito Speranza,^{§,‡} and Alfonso Grassi^{*,†,‡}

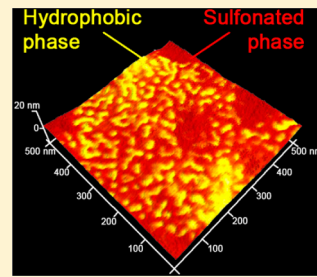
[†]Dipartimento di Chimica e Biologia, Università degli Studi di Salerno, via Ponte don Melillo, 84084 Fisciano (SA), Italy

[‡]NANOMATES, Research Centre for NANOMaterials and nanoTEchnology at Salerno University, 84084 Fisciano (SA), Italy

[§]Dipartimento di Ingegneria Industriale, Università degli Studi di Salerno, via Ponte don Melillo, 84084 Fisciano (SA), Italy

Supporting Information

ABSTRACT: The selective and quantitative sulfonation of polybutadiene (PB) and triblock copolymers polystyrene-*b*-polybutadiene-*b*-polystyrene (SBS) has been successfully obtained through a novel procedure consisting of two reaction steps carried out in a single batch: free radical addition of thiolacetic acid to olefinic double bonds followed by autocatalytic oxidation of the thioacetylated polymer with *in situ* generated organic peracids. The polymers resulting from the two reactions were fully characterized by NMR, FTIR, and elemental analysis; the ion exchange capacity (IEC) of the sulfonated polymers was assessed by elemental analysis and titration with NaOH. Critical desulfonation temperatures of the poly(alkylsulfonate)s were observed in the range 160–270 °C, whereas the thermal decomposition starts at about 380 °C. The TUNA-AFM analysis of a sample of SBS containing 79 mol % of alkylsulfonic groups showed a phase-separated morphology consisting of polystyrene domains of about 28 nm embedded in the sulfonated polymer matrix.



INTRODUCTION

Polyelectrolytes and ionomers are high molecular weight polymers characterized by the presence of Brønsted acidic groups, such as sulfonic $-\text{SO}_3\text{H}$ and carboxylic groups $-\text{COOH}$, located along the main chain or onto side and/or end groups of the polymer backbone.¹ Polyelectrolytes consist of one polar monomer whereas ionomers are typically block copolymers in which functionalized polymer segments spans apolar segments.² These polymers find application as superacid catalysts, sealing agents, adhesives, emulsifiers, compatibilizers and in the production of PEMs for fuel cells (PEMFCs).^{2–4} Typical examples are arylsulfonated polymers such as sulfonated poly(ether ether ketone), poly(ether sulfone), poly(ether sulfone ketone), poly(phenyl sulfone), polyimide, polybenzimidazole, and poly(phenylene oxide) which show arylsulfonic acid groups randomly distributed along the polymer chain.⁵ These polymers are strong Brønsted acids exhibiting thermal desulfonation in the temperature range 200–300 °C.

The current technology for PEMFCs is mainly based on perfluorosulfonic acid membranes which combine excellent thermal stability, chemical inertness, and good proton exchange capacity. Nafion,⁶ a random copolymer of tetrafluoroethylene and perfluorovinyl ethers patented by DuPont carrying perfluoroalkylsulfonic groups onto side groups of the main chain, is currently the most commercially relevant polymer for the production of PEMFCs.^{4b} This polymer exhibits excellent thermal stability, with a desulfonation temperature of 280–335 °C and pK_a of about –6.⁷ Factors severely limiting its extensive application are the cost, the high permeability to the solvents, and the low proton conductivity at low hydration degree.⁸

Thus, the synthesis of cheaper hydrocarbon-based sulfonated polymers showing comparable physical chemical properties is a topic of growing interest.

Even less thermally stable and weaker Brønsted acid, polyalkylsulfonates are useful in the same fields of application of polyarylsulfonates.⁹ Polybutadiene (PB) and butadiene-*co*-styrene polymers (SBR) are cheap and commercially available polymers suitable for the synthesis of polyelectrolytes and ionomers if a selective and efficient sulfonation procedure is available. A variety of synthetic methodologies have been reported in the patent and academic literature for the random sulfonation of polymers: (i) sulfur trioxide in vapor phase¹⁰ or in solution, possibly in presence of Lewis bases as triethyl phosphate,¹¹ tetrahydrofuran, dioxane, or amines;¹² (ii) chlorosulfonic acid in diethyl ether;¹³ (iii) concentrated sulfuric acid¹⁴ or mixtures of sulfuric acid with alkyl hypochlorite;¹⁵ (iv) bisulfites¹⁶ combined to dioxygen, hydrogen peroxide, metallic catalysts, or peroxy derivates;¹⁷ (v) acetyl sulfate.¹⁸

Most of the above-described methods are not environmentally friendly since they employ aggressive chemicals as SO_3 or H_2SO_4 and suffer the strong limitation of producing random and not selective sulfonation along the polymer chain.

In this paper we describe a cheap, fast, and selective synthetic route which allows sulfonation of olefinic $\text{C}=\text{C}$ double bond located in the main chain as well as in the side or end groups of the polymer chain. In addition, it avoids covalent cross-linking between the polymer chains and leaves notably the aromatic

Received: September 19, 2012

Revised: January 21, 2013

Published: February 1, 2013



Table 1. Synthesis of PB-TA and S(B-TA)S

entry ^a	polymer ^b	C=C:TAA:BZP (molar ratios)	time (h)	functionalization degree of olefinic C=C double bonds ^c		
				¹ H NMR (mol %)	(equiv/kg)	EA (equiv/kg)
1 ^d	PB	1:2:0	8	96	7.55	7.87
2 ^d	SBS	1:1:0	24	87	5.89	n.d.
3	PB	1:1.1:120	1	>99	7.68	7.54
4	SBS	1:1:120	1	91	6.02	5.48
5	SBS	1:2:120	1	96	6.12	5.47
6	SBS	1:1:40	1	95	6.12	5.74
7	SBS	1:1.1:120	4	>99	6.33	n.d.

^aReactions carried out in toluene at 25 °C under irradiation with UV light (365 nm, 100 W). ^bPB = 1,4-*cis*-polybutadiene (85 mol % 1,4-*cis* units), SBS = polystyrene-*b*-polybutadiene-*b*-polystyrene triblock copolymer (79 mol % of butadiene units). ^cIn mol % and equiv/kg of olefinic C=C reacted with TAA, determined by ¹H NMR and elemental analysis (EA). ^dControl experiments without UV activation.

moieties, e.g., polystyrene segments, totally unaffected. Polyalkylsulfonated block copolymers are thus synthesized with an eco-sustainable approach that employs nontoxic reagents, such as thiolacetic acid and *in situ* generated organic peracids.

EXPERIMENTAL SECTION

Materials. The manipulation of air- and moisture-sensitive compounds was performed under a nitrogen atmosphere using standard Schlenk techniques and a MBraun glovebox. Toluene (Carlo Erba, 99.5%) was used as received or predried with calcium chloride, refluxed for 48 h over sodium, and distilled before use in moisture- and oxygen-sensitive reactions. *cis*-1,4-Polybutadiene (PB; M_w = 495 kDa; cis-1,4-units = 85 mol %; 1,2-vinyl = 15 mol %) was synthesized as previously described.¹⁹ Polystyrene-*b*-polybutadiene-*b*-polystyrene (SBS; M_w = 86 kDa; S = 21 mol %; 1,4-units = 71 mol %; 1,2-vinyl = 8 mol %; Sigma-Aldrich), thiolacetic acid (TAA; 96%, Sigma-Aldrich), benzophenone (BZP; >99%, Sigma-Aldrich), formic acid (98%, Carlo Erba), hydrogen peroxide (35 wt % in water, Carlo Erba), potassium bromide (Sigma-Aldrich), silver paste (Sigma-Aldrich; 10 wt % dispersion of silver nanoparticles (<100 nm) in ethylene glycol), indium tin oxide (ITO)-coated glass slide (Sigma-Aldrich, 8–12 Ω/sq), dimethyl-*d*₆ sulfoxide (DMSO-*d*₆; Euriso-top), and 1,1,2,2-tetrachloroethane-*d*₂ (TCDE; Euriso-top) were used as received.

Measurements and Characterizations. NMR spectra were recorded on AVANCE Bruker spectrometers (400 and 300 MHz for ¹H): the chemical shifts are referenced to tetramethylsilane (TMS) as external reference, using the residual protio signal of the deuterated solvents. Elemental analysis was carried out on a CHNS Thermo Scientific Flash EA 1112 equipped with a thermal conductivity detector. FTIR measurements were performed using a Bruker Vertex 70 spectrometer equipped with deuterated triglycine sulfate detector and a Ge/KBr beam splitter. The samples were deposited from solutions over KBr disks or analyzed as films by casting. DSC analysis was carried out on a TA Instrument DSC 2920 calorimeter (heating rate = 10 °C/min). The thermogravimetric (TGA) and TGA-FTIR measurements were performed on a Netzsch TG 209 F1 (heating rate = 10 °C/min) coupled with a Bruker Vertex 70 FTIR spectrometer by means of a PTFE transfer line and a gas cell thermostated at 200 °C. The acquisition run consists of 30 scans in 28 s, with a resolution of 2 cm⁻¹ and a delay of 2 s between the runs. For the thioacetylation reaction the polymer solutions were irradiated at 365 nm in a UV incubator Bio-Link BLX (Vilber Lourmat). The ion exchange capacity (IEC) of the sulfonated polymers was determined by titration with standard solution of sodium hydroxide using the following method. Weighed amounts of the polymers were kept for 48 h under vigorous stirring in water and then titrated with NaOH (0.1 N) until to reach a persistent color of phenolphthalein used as indicator. Gel permeation chromatography (GPC) analysis of the polymers was carried out on a Breeze System (Waters) equipped with RI and UV-vis detectors

linearly connected to four columns packed with Styragel (particle size = 10 μm) using THF as eluent at 1.0 mL/min. The calibration was performed with polystyrene standards of M_w in the range of 10⁶–10² Da. Atomic force microscopy (AFM) images of thin films were collected in air at room temperature with a Dimension 3100 coupled with a Bruker Nanoscope V controller operating in tapping mode (TM-AFM) or in tunneling current mode (TUNA-AFM). The specimens to be analyzed were obtained by spin-coating of dimethyl sulfoxide (DMSO) solutions (30 μL; 0.2 wt %) at 80 °C onto glass slides using a speed rate of 1500 rpm and acceleration of 2000 rpm/s for 30 s. Commercial probe tips with nominal spring constants of 20–100 N m⁻¹, resonance frequencies in the range of 200–400 kHz, and tip radius of 5–10 nm were used. The TUNA-AFM measurements were performed using platinum-coated probes with nominal spring constants of 35 N m⁻¹ and electrically conductive tip of 20 nm. The samples were deposited from DMSO solutions (0.2 wt %; 10 μL; 80 °C) onto glass slide coated with ITO and electrically connected to the nanoscope with silver paste and aluminum foils. The support was heated at 250 °C for 1 h before the polymer deposition (see also Figure S19), and the specimen was annealed at 110 °C for 15 min before TUNA-AFM analysis. The images were analyzed using the Bruker software Nanoscope Analysis v1.40 r2sr1.

Synthesis of Sulfonated Polybutadiene by Free Radical Addition of Thiolacetic Acid Followed by *in Situ* Oxidation with Performic Acid. A representative procedure is given as follows. PB (8.000 g) was dissolved in toluene (800 mL) under vigorous stirring for 72 h at room temperature in a 1 L round-bottom flask. Benzophenone (BZP) (0.225 g; 1.23 mmol; BZP/olefin molar ratio = 1:120) and TAA (11.9 mL; 0.163 mol, TAA/olefin molar ratio = 1.1) were introduced into the reactor, and the polymer solution was irradiated for 1 h at room temperature with UV light of 365 nm and power of 100 W. The resulting thioacetylated polybutadiene (PB-TA; entry 3 of Table 1) was isolated by pouring 200 mL of the toluene solution in a plenty of methanol and the polymer recovered by filtration, washed with fresh methanol, and dried in vacuo at room temperature. Yield = 3.54 g. Formic acid (117 mL; 3.06 mol; HCOOH/olefin molar ratio = 25) were added to the toluene solution of PB-TA at 50 °C followed by slow addition of 52.6 mL of hydrogen peroxide (35 wt %; 0.61 mol; H₂O₂/olefin molar ratio = 5) in 20 min. CAUTION: the reaction is autocatalytic and strongly exothermic! The resulting slurry was stirred for 1 h, and the sulfonated polybutadiene (PB-SA; entry 8 of Table 3) was recovered by filtration, washed with acetonitrile, and dried in vacuo at 35 °C. Yield = 14.65 g.

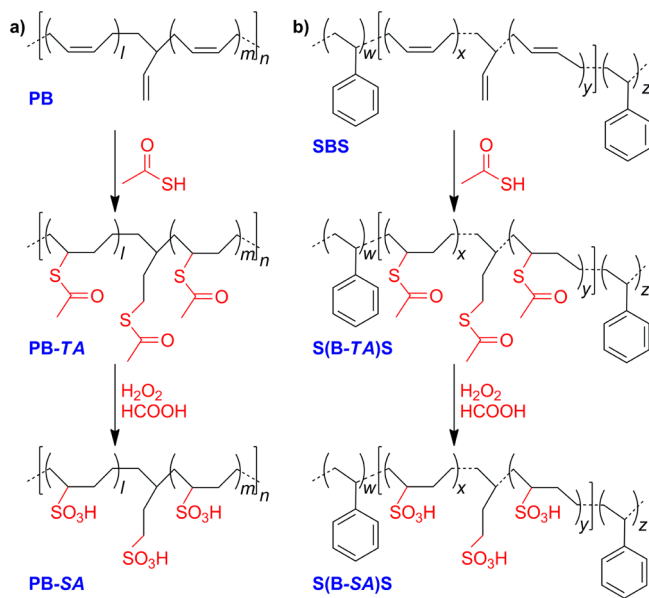
Synthesis of Sulfonated SBS by Free Radical Addition of Thiolacetic Acid Followed by *in Situ* Oxidation with Performic Acid. A representative procedure is given as follows. SBS (8.000 g) in toluene (800 mL) was left under vigorous stirring for 72 h at room temperature and heated later on for 1 h at 65 °C in a 1 L round-bottom flask until the complete dissolution of the polymer. Thus, BZP (0.173 g; 0.950 mmol; BZP/olefin molar ratio = 1:132) and TAA (8.02 mL; 0.114 mol, TAA/olefin molar ratio = 1.1) were added, and the polymer solution was irradiated for 4 h at room temperature with

UV light of 365 nm and power of 100 W. To isolate a fraction of the thioacetylated sample (S(B-TA)S; entry 7 of Table 1), 20 mL of the polymer solution was treated with plenty of methanol, and the polymer was recovered by filtration, washed with fresh methanol, and dried in vacuo at room temperature. The toluene solution containing the thioacetylated polymer was equilibrated at 50 °C, and 107.4 mL of formic acid (2.84 mol; HCOOH/olefin molar ratio = 27.5) and 48.9 mL of hydrogen peroxide (35 wt %; 0.57 mol; H₂O₂/olefin molar ratio = 5.5) were added in about 15 min. CAUTION: *the reaction is autocatalytic and strongly exothermic!* The resulting slurry was stirred for 1 h, and then most of the solvent was distilled off in vacuo at 35 °C. Aliquots of acetonitrile were added and subsequently distilled off in order to remove formic acid. Finally, the polymer (S(B-SA)S; entry 9 of Table 3) was coagulated in a plenty of acetonitrile, isolated by filtration, washed with fresh acetonitrile, and dried in vacuo at 35 °C. Yield = 15.92 g.

RESULTS AND DISCUSSION

Polybutadiene (PB) and polystyrene-*b*-polybutadiene-*b*-polystyrene triblock copolymer (SBS) were converted into the corresponding alkylsulfonated derivatives (PB-SA and S(B-SA)S) using the procedure in Scheme 1, which comprises of

Scheme 1. Synthetic Strategy for the Sulfonation of (a) PB and (b) SBS



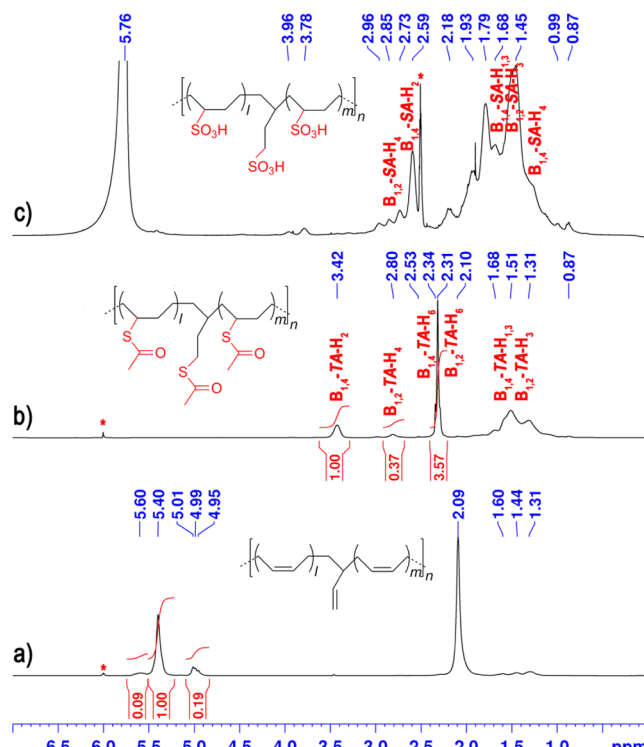
two reactions: (i) addition of thiolacetic acid (TAA) to the olefinic C=C double bonds to yield the thioacetylated polymers (PB-TA and S(B-TA)S); (ii) in-situ oxidation of PB-TA and S(B-TA)S with peracids to yield PB-SA and S(B-SA)S. The two reactions were carried out in sequence in the same batch without isolating the reaction products.

The synthesis of low molecular weight alkylsulfonic acids from addition of TAA to solutions of 1-olefins was previously reported;²⁰ however, to the best of our knowledge, the extension of this procedure for the efficient functionalization of high molecular weight polymers is unprecedented.

Addition of TAA to PB was preliminary carried out by adding 2 equiv²¹ of the acid to a toluene solution of the polymer (10 g/L) at 25 °C. The reaction proceeds faster onto 1,2-vinyl units, producing a quantitative functionalization of these units in 2 h, and yields the completely functionalized

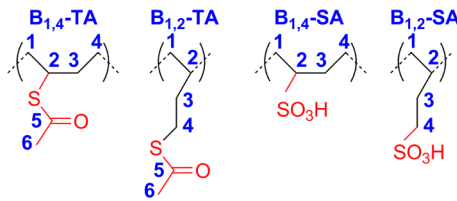
polymer PB-TA in 8 h (entry 1, Table 1, Table S1 and Figure S1).

Thioacetylation of SBS affords S(B-TA)S with a degree of functionalization of the olefinic C=C double bonds of 87 mol % in 24 h (entry 2, Table 1). When toluene solutions of SBS were additionally treated with 8 mequiv of benzophenone and irradiated with UV light ($\lambda = 365$ nm; 100 W), both PB-TA and S(B-TA)S were quantitatively obtained in only 1 h (entries 3 and 4, Table 1; see also Table S2 and Figure S2). The ¹H NMR spectrum of PB-TA shows the disappearance of the signals due to the olefinic protons and the presence of methyl signals at 2.31 ppm attributed to the thioacetyl group (Figure 1). Two



additional broad resonances at 3.42 and 2.80 ppm were respectively assigned to the methine protons B_{1,4'}-TA-H₂ (see Table 2) and methylene protons B_{1,2'}-TA-H₄, geminal to the sulfur atom, resulting from the addition of TAA to the cis-1,4 and 1,2-vinyl units, respectively. Noteworthy only the anti-Markovnikov addition product to 1,2-vinyl units was detected, in agreement with the radical reaction pathway previously reported at the surface of syndiotactic 1,2-polybutadiene films.²² The increase of the molar concentration of TAA (entry 5, Table 1) and BZP (entry 6, Table 1), as well as longer irradiation time, did not produce significant differences in the reaction rate.

The free radical addition of TAA to SBS produced the complete functionalization of the butadiene units in 4 h, leaving the styrene units totally unaffected (entry 7, Table 1). In the ¹H NMR spectrum of S(B-TA)S the same diagnostic ¹H signals described for PB-TA were actually observed (Figure S10). The chemical shifts of the diagnostic ¹³C NMR signals (Figure S3) were assigned by ¹H-¹³C HETCOR, HSQC, and DQF-COSY experiments (Figures S4-S6) and listed in Table 2. The degree

Table 2. ^1H and ^{13}C NMR Diagnostic Signals for PB-TA, PB-SA, S(B-TA)S, and S(B-SA)S

units	PB-TA ^b			S(B-TA)S ^b		PB-SA ^c		S(B-SA)S ^c	
	H/C	^1H (ppm)	^{13}C (ppm)	^1H (ppm)	^{13}C (ppm)	^1H (ppm)	^{13}C (ppm)	^1H (ppm)	^{13}C (ppm)
$\text{B}_{1,4}$	1,3	1.5	34.5	1.5	33.0	1.6	29.6	1.6	29.6
	2	3.42	44.2	3.46	42.9	2.59	59.8	2.62	60.1–59.8
	4	n.r. ^a	n.r.	n.r.	n.r.	1.36	23.9	1.36	23.9–23.6
	5		196		193				
	6	2.31	30.9	2.33	28.8				
$\text{B}_{1,2}$	3	1.46	23.9	1.4	22.4	1.64	30.3–28.3	1.69	30.3–28.3
	4	2.80	26.6	2.85	24.9	2.73	49.0	2.75	49.0
	5		196		193				
	6	2.31	30.9	2.33	28.8				

^an.r. = not resolved. ^bTetrachloroethane-*d*₂, 25 °C. ^cDimethyl-*d*₆ sulfoxide, 90 °C.

Table 3. Synthesis of PB-SA and S(B-SA)S

entry ^a	polymer	$\text{C}=\text{C:HCOOH:H}_2\text{O}_2$ (molar ratios)	sulfonation degree ^b		
			^1H NMR		EA (equiv/kg)
			(mol %)	(equiv/kg)	
8	PB-TA	1:25:5	>99	7.34	7.50
9	S(B-TA)S	1:27.5:5.5	>99	6.10	6.23

^aReactions carried out in toluene at 50 °C in 1 h. ^bIn mol % and equiv/kg of reacted olefinic C=C carbon bonds, determined by ^1H NMR, elemental analysis (EA) and titration with NaOH (IEC).

of functionalization of the olefinic carbon–carbon double bonds (Table 1) was assessed from the integral values of the ^1H and ^{13}C signals in S(B-TA)S (Figures S10 and S11), using the polystyrene segments as internal reference. Covalent cross-linking of the polymer chains was not observed during the free radical thioacetylation reaction; actually, the average molecular weight of sample 7 well compares with the value of the pristine polymer SBS (80 kDa vs 86 kDa) determined by GPC analysis.

Hence, PB-TA and S(B-TA)S were oxidized to the corresponding sulfonated polymer via autocatalytic oxidation with peracids generated *in situ* by a mixture of a carboxylic acid and hydrogen peroxide. A toluene solution of PB-TA was treated with excess of formic acid at 50 °C followed by drop-to-drop addition of an aqueous solution of hydrogen peroxide in 20 min: the expected PB-SA was obtained in high yield in 1 h (entry 8, Table 3). *Caution: the reaction is exothermic and autocatalytic because of the alkylsulfonic groups generated during the reaction!* When the oxidation of PB-TA was carried out using a mixture of hydrogen peroxide and acetic acid, the same degree of sulfonation of the unsaturated polymer was observed; however, an unpure polymer was recovered after the work-up because of the higher boiling point of acetic acid which makes harder the purification of the polymer by distilling off the volatiles.

The degree of sulfonation of PB-SA and S(B-SA)S, assessed by ^1H NMR spectroscopy and elemental analysis, was found higher than 99% for all of the investigated polymers (Table 3). In the ^1H NMR spectrum of PB-SA (Figure 1c) the broad signal at 2.59 ppm is attributed to the methine protons of the main chain carrying the sulfonic group,^{9b,18e} which is in turn

coupled to the two doublet of doublets of the adjacent methylene protons of the main chain observed at about 1.6 ppm (see Figure S9). The chemical shifts of the ^1H (Figure 1c and Figure S12) and ^{13}C NMR (Figures S7 and S13) diagnostic signals were attributed by means of two-dimensional ^1H – ^{13}C HETCOR and COSY experiments (see Figures S8 and S9) and are given in Table 2. In particular, the low-intensity signals at 2.73 and 1.64 ppm were respectively attributed to the methylene protons in geminal position ($\text{B}_{1,2}\text{-SA-H}_4$) or adjacent ($\text{B}_{1,2}\text{-SA-H}_3$) to the sulfonic group of 1,2-vinyl units.

The FTIR spectra of PB-TA (Figure 2b) and S(B-TA)S (Figure S14b) exhibit two signals at 1689 and 953 cm⁻¹ attributed to the thioacetyl moiety (compare Figures 2a and 2b);^{23a} these signals were replaced by vibrations at 1334, 1180, 1036, and 861 cm⁻¹ characteristic of the sulfonic acid groups²³ in PB-SA (Figure 2c) and S(B-SA)S (Figure S14c; see also Table S3 for the complete FTIR assignments).

Considering the potential application of the thioacetylated and sulfonated polymer above-described for the production of PEMFCs, their physical properties were investigated. PB-TA and S(B-TA)S exhibit solubility comparable to the pristine polymers: they are completely soluble in typical organic solvents as toluene and chloroform, whereas are totally insoluble in polar solvents as acetonitrile, methanol, and water (see Table 4). On the contrary, PB-SA and S(B-SA)S are soluble in DMSO and *N,N*-dimethylacetamide (DMAc) but insoluble in methanol, where they produce a slurry from which the polymers can be recovered by filtration with difficulty. Among the sulfonated derivatives only PB-SA resulted soluble in water.

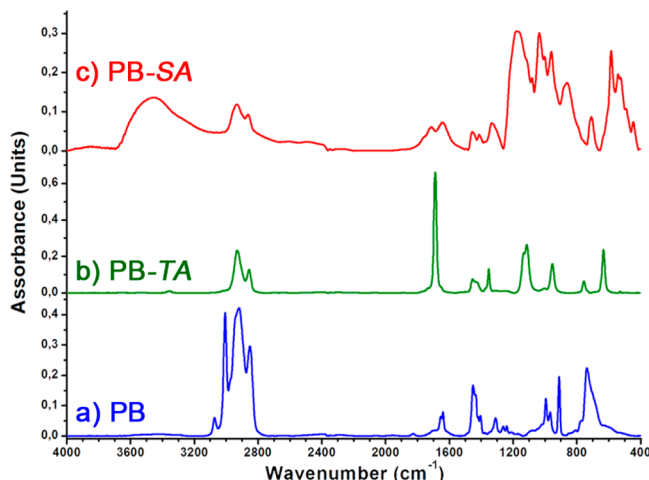


Figure 2. FTIR spectra of PB, PB-TA (entry 3, Table 1), and PB-SA (entry 8, Table 3).

The thermal stability of PB-TA, S(B-TA)S, PB-SA, and S(B-SA)S was investigated by differential scanning calorimetry (DSC) and thermogravimetric analysis coupled with FTIR (TGA-IR). The T_g value shifted from $-98.9\text{ }^\circ\text{C}$ of PB to -12.6 and $-27.9\text{ }^\circ\text{C}$ in PB-TA and PB-SA as a result of the reduced conformational mobility of the functionalized polymer chains (Figure 3).¹⁷ The alkylsulfonated PB-SA and S(B-SA)S showed thermal stability similar to that of arylsulfonated polymers.⁵ Two desulfonation temperature were actually found in the TGA-IR profiles at 159 and $235\text{ }^\circ\text{C}$ for PB-SA and at 228 and $270\text{ }^\circ\text{C}$ for S(B-SA)S (Figure 4 and Figures S15 and S16) whose origin is currently subject of further investigations. The overall weight fraction of the sulfonic groups evaluated by both ^1H NMR spectroscopy and EA was found in good agreement with the weight loss of the polymers after SO_2 evolution. The weight loss values of 67.3 and 49.1 wt \% for PB-SA and S(B-SA)S determined by TGA (see Figure S15), respectively, well compare with 60.0 and 49.4 wt \% predicted by ^1H NMR.

Tapping mode AFM (TM-AFM) allows evidencing the topological morphology in phase-separated materials. During the probe scanning the image contrast results from the different response of the phases at variance of mechanical, adhesion, friction, or other chemical–physical properties of the domains.^{19d,24} A spin-coated thin film of S(B-SA)S (entry 9, Table 3) by DMSO solution (0.2 wt \%), constituted of 79 mol \% of sulfonated PB, resulted flat at TM-AFM, without apparent evidence of phase-separated morphology (Figure 5a). However, the corresponding phase image, in Figure 5b, shows rigid domains as bright “hills” of about 28 nm in diameter embedded in a soft polymer matrix (see also Figures S17 and S18). One can speculate that the rigid phase consists of PS and the matrix of the sulfonated polymer domains; as a matter of fact, the

relative area values of the two domains are roughly comparable to those expected from the chemical composition of the sample (entry 9 of Table 3).²⁴ To confirm this attribution, a thin film of S(B-SA)S was deposited onto a glass support coated with ITO, electrically connected to the nanoscope holder by means silver paste and aluminum foil (Figure S19) and analyzed by tunneling current AFM (TUNA-AFM). This technique permits to characterize ultralow currents through the thickness of thin films employing a conductive probe tip that detects conductivity variations across medium- to low-conducting and semiconducting films. TUNA-AFM was shown to highlight proton conductive regions in organic and inorganic thin films.²⁵ When sample topography and tip–sample current are measured simultaneously, a direct correlation between the local morphology and the measured electrical properties becomes possible. In particular, conducting AFM was used to obtain high spatial resolution images of the current passing through each channel of a Nafion PEM in an electrochemically active fuel cell.^{25a} In this contest, Figure 5c and Figure S20 show TUNA-AFM image of S(B-SA)S where small non-conductive regions, comparable in size to the polystyrene domains observed in the TM-AFM image, are homogeneously dispersed in a conductive polymer matrix, covering $\sim 70\%$ of the surface (see Figure S20). These preliminary results allows us to confirm the phase-separated morphology in the thin films resulting from the sulfonated polymer produced with the procedure described in this paper and seem promising for the applications of these ionomers in PEMFC technology.

CONCLUSIONS

At the same concentration of sulfonic groups, sulfonated multiblock ionomers consisting of hydrophobic and hydrophilic polymer segments exhibit performances, e.g., in PEMs applications, higher than randomly sulfonated polymer.²⁶ Actually, the enhanced phase segregation assures better proton conductivity, increased mechanical properties, and lower permeability to the solvent.^{26,27} In this article we report on fast, selective, and single batch procedure which leads to the formal addition of a hydrogen atom and a sulfonic acid group to the olefinic carbon–carbon double bond located in the main chain or as side or end group of a polymer backbone. This result has been successfully obtained using an economical and eco-friendly synthetic approach. When applied to styrene–butadiene block copolymers, ionomers selectively functionalized in the alkyl regions of the polymer chain have been obtained without observing covalent cross-linkings among the macromolecules. The novel route provides a powerful tool for the synthesis of sulfonated block copolymers.

Table 4. Solubility of PB-TA, S(B-TA)S, PB-SA, and S(B-SA)S

polymer	solvent					
	toluene	chloroform	acetonitrile	DMSO ^a	DMAC ^b	water
PB-TA	soluble	soluble	insoluble	insoluble	insoluble	insoluble
S(B-TA)S	soluble	soluble	insoluble	insoluble	insoluble	insoluble
PB-SA	insoluble	insoluble	insoluble	soluble	soluble	soluble
S(B-SA)S	insoluble	insoluble	insoluble	soluble	soluble	insoluble

^aDimethyl sulfoxide. ^bN,N-Dimethylacetamide.

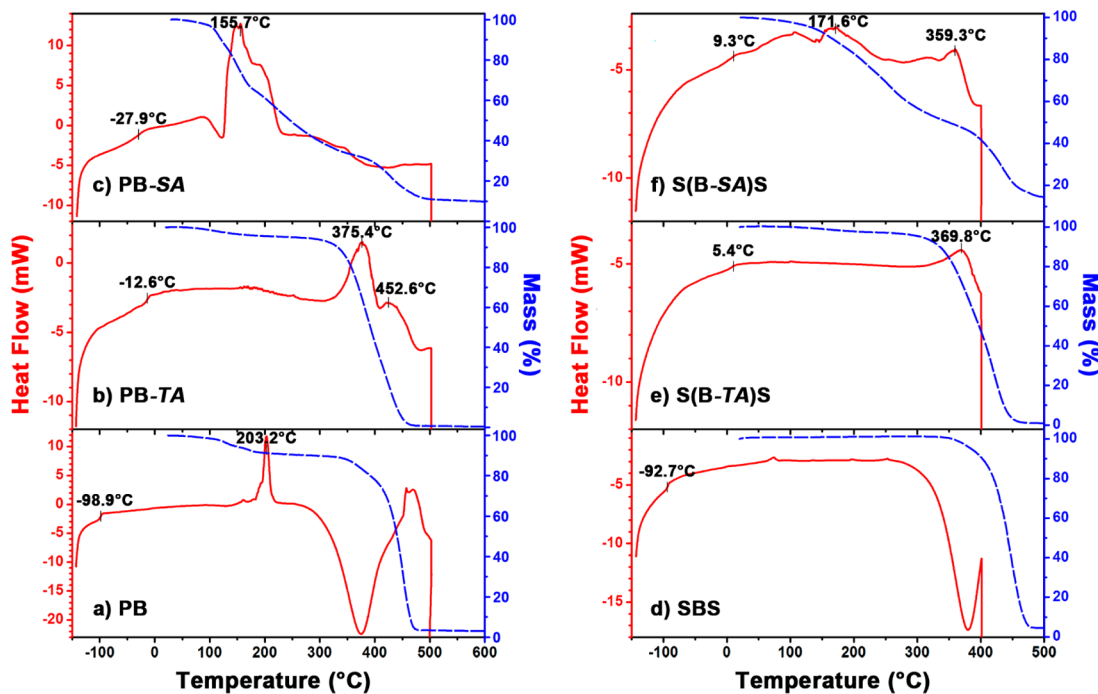


Figure 3. DSC (red curves) and TGA (blue dashed curves) traces of PB, PB-TA (entry 3, Table 1), PB-SA (entry 8, Table 3), SBS, S(B-TA)S (entry 7, Table 1), and S(B-SA)S (entry 9, Table 3).

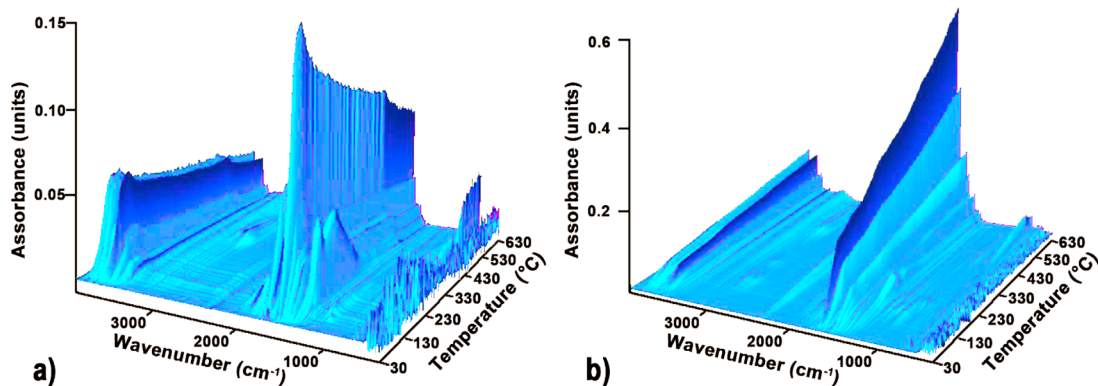


Figure 4. FTIR plots of the gas evolved during the thermal decomposition of (a) PB-SA (entry 8, Table 3) and (b) S(B-SA)S (entry 9, Table 3).

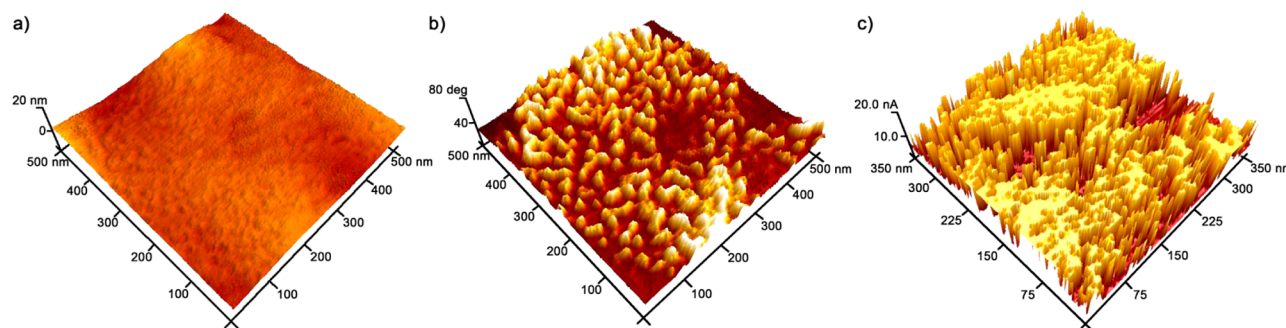


Figure 5. Thin film morphology of S(B-SA)S (sample 9, Table 3): TM-AFM height (a) and phase (b) images of a spin-coated film on glass; TUNA-AFM current image (c) of a thin film deposited on ITO-coated glass (dc sample bias = 2.5 V and current sensitivity of 1 pA/V).

ASSOCIATED CONTENT

Supporting Information

Experimental details, NMR, FTIR, TGA-IR, and AFM characterizations. This material is available free of charge via the Internet at <http://pubs.acs.org>.

AUTHOR INFORMATION

Corresponding Author

*E-mail: agrassi@unisa.it; Fax +39-089969824.

Notes

The authors declare no competing financial interest.

ACKNOWLEDGMENTS

Authors acknowledge the financial support from Ministero dell'Istruzione dell'Università e della Ricerca (MIUR, Roma - Italy; FARB-2009) and PON (Network of Excellence MASTRI) and are also grateful to Dr. Patrizia Oliva, Dr. Patrizia Iannece, and Dr. Ivano Immediata for technical assistance.

ABBREVIATIONS

BZP, benzophenone; DSC, differential scan calorimetry; DMAc, *N,N*-dimethylacetamide; DMSO, dimethyl sulfoxide; EA, elemental analysis; FTIR, Fourier transform infrared; GPC, gel permeation chromatography; ITO, indium tin oxide; PB, *cis*-1,4-polybutadiene; PB-SA, sulfonated polybutadiene; PB-TA, thioacetylated polybutadiene; PEMFC, polymer electrolyte membrane fuel cell; SBS, polystyrene-*b*-polybutadiene-*b*-polystyrene; S(B-TA)S, thioacetylated polystyrene-*b*-polybutadiene-*b*-polystyrene; S(B-SA)S, sulfonated polystyrene-*b*-polybutadiene-*b*-polystyrene; TAA, thiolacetic acid; TCDE, 1,1,2,2-tetrachloroethane-*d*₂; TGA, thermogravimetric analysis; TMAFM, tapping mode atomic force microscopy; TUNA-AFM, tunneling current atomic force microscopy.

REFERENCES

- (1) Koetz, J.; Kossmella, S. *Polyelectrolytes and Nanoparticles*; Springer: Berlin, 2007.
- (2) Grady, B. P. *Polym. Eng. Sci.* **2008**, *48*, 1029–1051.
- (3) (a) Olah, G. A.; Prakash, G. K. S.; Molnár, A.; Sommer, J. *Superacid Chemistry*; John Wiley & Sons, Inc.: Hoboken, NJ, 2009. (b) Barbaro, P.; Liguori, F. *Chem. Rev.* **2008**, *109*, 515–529. (c) Gelbard, G. *Ind. Eng. Chem. Res.* **2005**, *44*, 8468–8498.
- (4) (a) Zhang, H.; Shen, P. K. *Chem. Rev.* **2012**, *112*, 2780–2832. (b) Zhang, H.; Shen, P. K. *Chem. Soc. Rev.* **2012**, *41*, 2382–2394.
- (5) Hou, H.; Di Vona, M. L.; Knauth, P. *ChemSusChem* **2011**, *4*, 1526–1536.
- (6) Mauritz, K. A.; Moore, R. B. *Chem. Rev.* **2004**, *104*, 4535–4586.
- (7) Ulbricht, M. *Polymer* **2006**, *47*, 2217–2262.
- (8) Roh, D. K.; Koh, J. K.; Chi, W. S.; Shul, Y. G.; Kim, J. H. *J. Appl. Polym. Sci.* **2011**, *121*, 3283–3291.
- (9) (a) Asano, N.; Aoki, M.; Suzuki, S.; Miyatake, K.; Uchida, H.; Watanabe, M. *J. Am. Chem. Soc.* **2006**, *128*, 1762–1769. (b) Saito, J.; Miyatake, K.; Watanabe, M. *Macromolecules* **2008**, *41*, 2415–2420. (c) Miyatake, K.; Furuya, H.; Tanaka, M.; Watanabe, M. *J. Power Sources* **2012**, *204*, 74–78. (d) Sheng, L.; Higashihara, T.; Nakazawa, S.; Ueda, M. *Polym. Chem.* **2012**, *3*, 3289–3295. (e) Yin, Y.; Du, Q.; Qin, Y.; Zhou, Y.; Okamoto, K. *J. Membr. Sci.* **2011**, *367*, 211–219. (f) Chang, Y.; Brunello, G. F.; Fuller, J.; Hawley, M.; Kim, Y. S.; Disabb-Miller, M.; Hickner, M. A.; Jang, S. S.; Bae, C. *Macromolecules* **2011**, *44*, 8458–8469.
- (10) Moody, H. R.; Edwards, R. W. Vapor Phase Sulfonation of Polymer Particles. U.S. Patent 3,218,301, November 16, 1965.
- (11) Stratton, C. A. Method for Sulfonating *cis* 1,4-Polybutadiene. U.S. Patent 3,432,480, March 11, 1969.
- (12) Canter, N. H. Sulfonated Polymers. U.S. Patent 3,642,728, February 15, 1972.
- (13) O'Neil, W. P.; Turner, W. V. Selectively Sulfonated Block Copolymers and Process for Their Preparation. U.S. Patent 3,642,953, February 15, 1972.
- (14) (a) Zimmermann, A.; Tauer, K. Verfahren zur Herstellung von wässrigen Polymerdispersionen mit wasserlöslichen Polyoleinstabilisatoren. German Patent DE 100 22 871 A1, November 15, 2001. (b) Tauer, K.; Zimmermann, A. *Macromol. Rapid Commun.* **2000**, *21*, 825–831.
- (15) Sakuragi, T.; Akiyama, S. Manufacture of High Molecular Weight Substance. U.S. Patent 3,551,394, December 29, 1970.
- (16) (a) Matsuda, Y.; Suzuki, Y.; Yasui, S. Sulfonated Product of Butadiene or Isoprene and the Production Thereof. U.S. Patent 4,115,437, September 19, 1978. (b) Lee, B.; Pielartzik, H.; Jacobs, G. Sulfonated Aliphatic Compounds. U.S. Patent 5,919,976, July 6, 1999.
- (17) Nandi, A.; M. Gupta, D.; Banthia, A. K. *Macromol. Rapid Commun.* **1999**, *20*, 582–585.
- (18) (a) Makowski, H. S. Process for Forming a Barium Sulfonate Containing Polymer. U.S. Patent 4,310,445, January 12, 1982. (b) Balas, J. G.; Gergen, W. P. Sulfonated Block Copolymers. U.S. Patent 5,239,010, August 24, 1993. (c) Zhang, X.; Liu, S.; Liu, L.; Yin, J. *Polymer* **2005**, *46*, 1719–1723. (d) Zhao, Y.; Yin, J. *J. Membr. Sci.* **2010**, *351*, 28–35. (e) Zhao, Y.; Yin, J. *Eur. Polym. J.* **2010**, *46*, 592–601.
- (19) (a) Oliva, L.; Longo, P.; Grassi, A.; Ammendola, P.; Pellecchia, C. *Makromol. Chem., Rapid Commun.* **1990**, *11*, 519–524. (b) Grassi, A.; Buonerba, A. Sintesi di Polialchilosolfonati da Destinare alla Produzione di Ionomeri e Polielettroliti Mediante Solfonazione Selettiva di Polidieni e Copolimeri dei Dieni Coniugati, Italian Patent. SA2012A000007, May 16, 2012. (c) Buonerba, A.; Cuomo, C.; Ortega Sánchez, S.; Canton, P.; Grassi, A. *Chem.—Eur. J.* **2012**, *18*, 709–715. (d) Buonerba, A.; Cuomo, C.; Speranza, V.; Grassi, A. *Macromolecules* **2010**, *43*, 367–374.
- (20) Showell, J. S.; Russell, J. R.; Swern, D. *J. Org. Chem.* **1962**, *27*, 2853–2858.
- (21) The equivalents are calculated with reference to the olefinic C=C double bonds.
- (22) Mumbauer, P. D.; Carey, D. H.; Ferguson, G. S. *Chem. Mater.* **1995**, *7*, 1303–1314.
- (23) (a) Nyquist, R. A. *Interpreting Infrared, Raman, and Nuclear Magnetic Resonance Spectra*; Elsevier: Amsterdam, 2001. (b) Silverstein, R. M.; Webster, F. X.; Kiemle, D. J. *Spectrometric Identification of Organic Compounds*; John Wiley & Sons: New York, 2008. (c) Opper, K. L.; Wagener, K. B. *Macromol. Rapid Commun.* **2009**, *30*, 915–919.
- (24) (a) Knoll, A.; Magerle, R.; Krausch, G. *Macromolecules* **2001**, *34*, 4159–4165. (b) Wang, D.; Fujinami, S.; Liu, H.; Nakajima, K.; Nishi, T. *Macromolecules* **2010**, *43*, 9049–9055.
- (25) (a) Bussian, D. A.; O'Dea, J. R.; Metiu, H.; Buratto, S. K. *Nano Lett.* **2007**, *7*, 227–232. (b) Park, J. Y.; Maier, S.; Hendriksen, B.; Salmeron, M. *Mater. Today* **2010**, *13*, 38–45. (c) Tercjak, A.; Gutierrez, J.; Ocando, C.; Mondragon, I. *Langmuir* **2010**, *26*, 4296–4302.
- (26) (a) Elabd, Y. A.; Hickner, M. A. *Macromolecules* **2011**, *44*, 1–11. (b) Li, N.; Hwang, D. S.; Lee, S. Y.; Liu, Y.-L.; Lee, Y. M.; Guiver, M. D. *Macromolecules* **2011**, *44*, 4901.
- (27) Bose, S.; Kuila, T.; Nguyen, T. X. H.; Kim, N. H.; Lau, K.-t.; Lee, J. H. *Prog. Polym. Sci.* **2011**, *36*, 813–843.

Supporting Information

**Novel Synthetic Strategy for the Sulfonation of
Polybutadiene and Styrene-Butadiene Copolymers**

Antonio Buonerba,^{†,‡} Vito Speranza^{§,‡} and Alfonso Grassi*,^{†,‡}

[†]Dipartimento di Chimica e Biologia, Università degli Studi di Salerno, via Ponte don Melillo,
84084 Fisciano (SA), Italy,

[‡]NANOMATES, Research Centre for NANOMaterials and nanoTEchnology at Salerno
University, 84084 Fisciano (SA), Italy,

[§]Dipartimento di Ingegneria Industriale, Università degli Studi di Salerno, via Ponte don
Melillo, 84084 Fisciano (SA), Italy.

*e-mail: agrassi@unisa.it

Table of contents.

1. SUPPLEMENTARY EXPERIMENTAL DETAIL	5
1.1. Synthesis of PB-TA by addition of TAA to PB (entry 1, Table 1).	5
1.2. Synthesis of S(B-TA)S (entry 2, Table 1).	5
1.3. Synthesis of S(B-TA)S under irradiation with UV light (365 nm - 100 W): effect of the irradiation time (entry 4, Table 1).	5
1.4. Synthesis of S(B-TA)S under irradiation with UV light (365 nm - 100 W): effect of the concentration of TAA (entry 5, Table 1).	6
1.5. Synthesis of S(B-TA)S under irradiation with UV light (365 nm - 100 W): effect of the concentration of BZP (entry 6, Table 1).	6
2. KINETICS OF TAA ADDITION	7
2.2. Kinetics of TAA addition to PB.	7
Table S1. Addition of TAA to PB (entry 1, Table 1).	7
Figure S1. Plot of TAA addition to PB (entry 1, Table 1 and S1).	7
2.2. Kinetics of TAA addition to SBS activated with BZP and UV light.	8
Table S2. Addition of TAA to SBS (entry 4, Table 1).	8
Figure S2. Plot of TAA addition to SBS activated with BZP and irradiation with UV light (entry 4, Table 1 and S2).	8
3. NMR CHARACTERIZATION	9
3.1. ^{13}C NMR spectrum of PB-TA.	9
Figure S3. a) ^{13}C NMR spectrum (TCDE, 25°C) of PB-TA (entry 3, Table 1); b) magnification of the 50-14 ppm spectral region.....	9
3.2. DEPT135- ^1H -HETCOR spectrum of PB-TA.....	10
Figure S4. ^1H / ^{13}C -DEPT135 HETCOR spectrum (300 MHz, TCDE, 25°C) of PB-TA (entry 3, Table 1).	10
3.3. ^1H - ^{13}C HSQC spectrum of PB-TA.....	11
Figure S5. ^1H - ^{13}C HSQC spectrum (400 MHz, TCDE; 25°C) of PB-TA (entry 3, Table 1); the correlation spots due to methyl and methine signals are in blue, methylene in red	11
3.4. ^1H - ^1H DQF-COSY spectrum of PB-TA.....	12
Figure S6. ^1H - ^1H DQF-COSY spectrum (250 MHz, TCDE, 25°C) of PB-TA (entry 3, Table 1).	12
3.5. ^{13}C NMR spectrum of PB-SA.....	13

Figure S7. a) ^{13}C NMR spectrum (300 MHz, $^*\text{DMSO-d}_6$, 90°C) of PB-SA (entry 8, Table 3); b) magnification of the 70–20 ppm spectral region.....	13
3.6. DEPT135- ^1H HETCOR spectrum of PB-SA	14
Figure S8. ^1H - ^{13}C -DEPT135 HETCOR spectrum (300 MHz, $^*\text{DMSO-d}_6$, 90°C) of PB-SA (entry 8, Table 3).....	14
3.7. ^1H - ^1H DQF-COSY spectrum of PB-SA	15
Figure S9. ^1H - ^1H DQF-COSY spectrum (250 MHZ, $^*\text{DMSO-d}_6$, 90°C) of PB-SA (entry 8, Table 3)	15
3.8. ^1H NMR spectrum of S(B-TA)S.....	16
Figure S10. ^1H -NMR spectra (400 MHz, $^*\text{TCDE}$, 25°C) of: a) SBS and b) S(B-TA)S (entry 4, Table 1). The characteristic signals of polystyrene were not labelled for simplicity.....	16
3.9. ^{13}C NMR spectrum of S(B-TA)S.....	17
Figure S11. a) ^{13}C -NMR spectrum (TCDE, 25°C) of S(B-TA)S (entry 7, Table 1); b)magnification of the region 50-14 ppm (black curve) and of the DEPT135 spectrum (red curve). The characteristic signals of polystyrene were not labelled for simplicity.....	17
3.10. ^1H NMR spectrum of S(B-SA)S.....	18
Figure S12. ^1H NMR spectrum (300 MHz, DMSO-d ₆ /TCDE, v/v = 3:1, 90°C) of S(B-TA)S (entry 9, Table 3). The characteristic signals of polystyrene were not labelled for simplicity.....	18
3.11. ^{13}C NMR spectrum of S(B-SA)S.....	19
Figure S13. a) ^{13}C NMR spectrum (DMSO-d ₆ /TCDE, v/v = 3:1, 90°C) of S(B-SA)S (entry 9, Table 3); b) magnification of the region 50-14 ppm (black curve) and of the DEPT135 spectrum (red curve). The characteristic signals of polystyrene were not labelled for simplicity.....	19
4. FTIR CHARACTERIZATION	20
4.1. FTIR spectra of SBS, S(B-TA) and S(B-SA)S	20
Figure S14. FTIR spectra of: a) SBS; b) S(B-TA)S (entry 7, Table 1); c) S(B-SA)S (entry 9, Table 3)	20
4.2. FTIR assignments.....	21
Table S3. Main FTIR vibration assignments	21
5.TGA and TGA-IR CHARACTERIZATION	22
Figure S16. Plot of SO ₂ thermal evolution by TGA-IR (signals at 1345 cm ⁻¹) from: a) PB-SA (entry 8, Table 3); b) S(B-SA)S (entry 9, Table 3)	23

6. AFM Analysis of S(B-SA)S.....	24
6.1. Dimension Distribution Analysis of PS domains in thin films of S(B-SA)S.....	24
Figure S17. TM-AFM phase images of S(B-SA)S (entry 9, Table 3; scan size = 500 nm, z-scale = 80 deg): a) as acquired; b) with PS domains highlighted for the dimension distribution analysis performed with Nanoscope Analysis v1.40 r2sr1 software from Bruker.....	24
Figure S18. Dimension distribution analysis of PS domains of Figure S17 b.....	24
6.2. TUNA-AFM characterization of thin films of S(B-SA)S.....	25
Figure S19. a) Schematic representation of the conductive support for TUNA-AFM measurements. b) The device.....	25
Figure S20. 2D TUNA-AFM micrographs of S(B-SA)S (entry 9, Table 3) corresponding to the image in Figure 5 c: a) height image (scan size = 350 nm, z-scale = 40 nm); b) TUNA Current (scan size = 350 nm, z-scale = 20 nA).	25

1. SUPPLEMENTARY EXPERIMENTAL DETAIL.

1.1. Synthesis of PB-TA by addition of TAA to PB (entry 1, Table 1).

PB (4.00g) and toluene (400 mL) were introduced in a 500 mL flask and left under vigorous stirring for 72 hours. 10.85 mL of TAA (0.15 mol; TAA/olefin molar ratio = 2) were added to the solution and the reaction was monitored by sampling hourly aliquots of 20 mL in 8 hours. The polymers were coagulated by pouring the solutions in a plenty of methanol and the derivatives were recovered by filtration, washed with methanol and dried in vacuum at room temperature (see also **Table S1** and **Figure S1**).

1.2. Synthesis of S(B-TA)S (entry 2, Table 1).

SBS (5.00 g) and toluene (500 mL) were left under vigorous stirring for 72 hours at room temperature in a 1 L flask. Thus 4.47 mL of TAA (61 mmol, TAA/olefin molar ratio = 1) were added to the solution and left to react for 24 h at room temperature. The polymer was coagulated in methanol, recovered by filtration, washed with fresh methanol and dried in vacuo at room temperature.

1.3. Synthesis of S(B-TA)S under irradiation with UV light (365 nm - 100 W): effect of the irradiation time (entry 4, Table 1).

Four 20 mL glass vials were each charged with 10 mL of a toluene solution of SBS (10 g/L), 1.85 mL of a toluene solution of BZP (2.0 g/L; 0.010 mmol; BZP/olefin molar ratio = 1:120) and 96 μ L of TAA (1.22 mmol; TAA/olefin molar ratio = 1). The vials were sealed and exposed to UV light at 365 nm and power of 100 W for 5s, 5min, 30min and 60min. The polymers were recovered by coagulation in methanol, isolated by filtration, washed with methanol and dried in vacuo at room temperature (see also Table S2 and Figure S2).

1.4. Synthesis of S(B-TA)S under irradiation with UV light (365 nm - 100 W): effect of the concentration of TAA (entry 5, Table 1).

A 20 mL glass vial was charged with 10 mL of a toluene solution of SBS (10 g/L), 1.85 mL of a toluene solution of BZP (2.0 g/L; 0.010 mmol; BZP/olefin molar ratio = 1:120) and 192 μ L of TAA (2.44 mmol; TAA/olefin molar ratio = 2). The vial was sealed and exposed to UV light at 365 nm and power of 100 W for 60 min. S(B-TA)S was recovered by coagulation in methanol, isolated by filtration, washed with methanol and dried in vacuo at room temperature.

1.5. Synthesis of S(B-TA)S under irradiation with UV light (365 nm - 100 W): effect of the concentration of BZP (entry 6, Table 1).

A 20 mL glass vial was charged with 10 mL of a toluene solution of SBS (10 g/L), 5.55 mL of a toluene solution of BZP (2.0 g/L; 0.030 mmol; BZP/olefin molar ratio = 1:40) and 96 μ L of TAA ($1.22 \cdot 10^{-3}$ mol; TAA /olefin molar ratio = 1). The vial was sealed and exposed to UV light at 365 nm and power of 100 W for 60 min. S(B-TA)S was recovered by coagulation in methanol, isolated by filtration, washed with methanol and dried in vacuo at room temperature.

2. KINETICS OF TAA ADDITION.

2.2. Kinetics of TAA addition to PB.

Table S1. Addition of TAA to PB (entry 1, Table 1).

Time ^{a)} [h]	1,4-PB ^{b)} [mol%]	1,2-PB ^{b)} [mol%]	1,4-PB-TA ^{b)} [mol%]	1,2-PB-TA ^{b)} [mol%]	$\Phi_{TA}^{b),c)}$ [mol%]
0	83.5	16.5	0	0	0
1	77.6	11.0	6.9	4.5	11.4
2	52.2	0.7	33.0	14.1	47.1
3	28.6	0	54.9	16.5	71.4
4	19.3	0	64.2	16.5	80.7
5	13.8	0	69.7	16.5	86.2
6	9.2	0	74.3	16.5	90.8
7	6.4	0	77.1	16.5	93.6
8	3.4	0	80.1	16.5	96.6
24	0	0	83.5	16.5	>99

^{a)}The reaction conditions are given in entry 1 of Table 1. ^{b)}Determined by ¹H NMR. ^{c)}Degree of functionalization of the olefinic units.

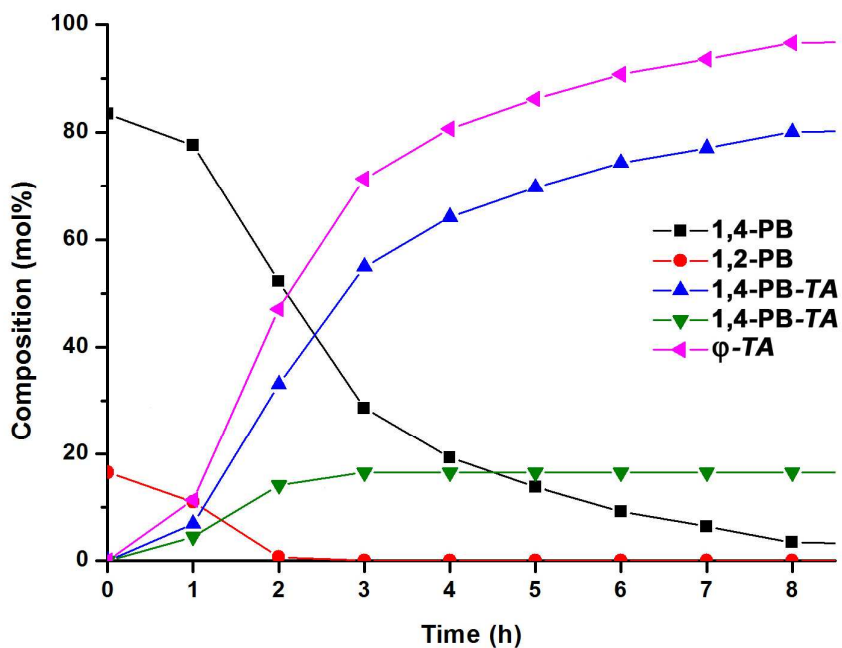


Figure S1. Plot of TAA addition to PB (entry 1, Table 1 and S1).

2.2. Kinetics of TAA addition to SBS activated with BZP and UV light.

Table S2. Addition of TAA to SBS (entry 4, Table 1).

Time ^{a)} [s]	1,4-PB ^{b)} [mol%]	1,2-PB ^{b)} [mol%]	1,4-PB-TA ^{b)} [mol%]	1,2-PB-TA ^{b)} [mol%]	$\Phi_{TA}^{b),c)}$ [mol%]
0	90.0	10.0	0	0	0
5	89.6	9.5	0.4	0.5	0.9
300	34.3	0.3	55.7	9.7	65.4
1800	11.7	0	78.3	10.0	88.3
3600	7.5	0	81.5	10.0	91.5

^{a)} The reaction conditions are given in entry 4 of Table 1. ^{b)} Determined by ¹H-NMR.

^{c)}Degree of functionalization of the olefinic units.

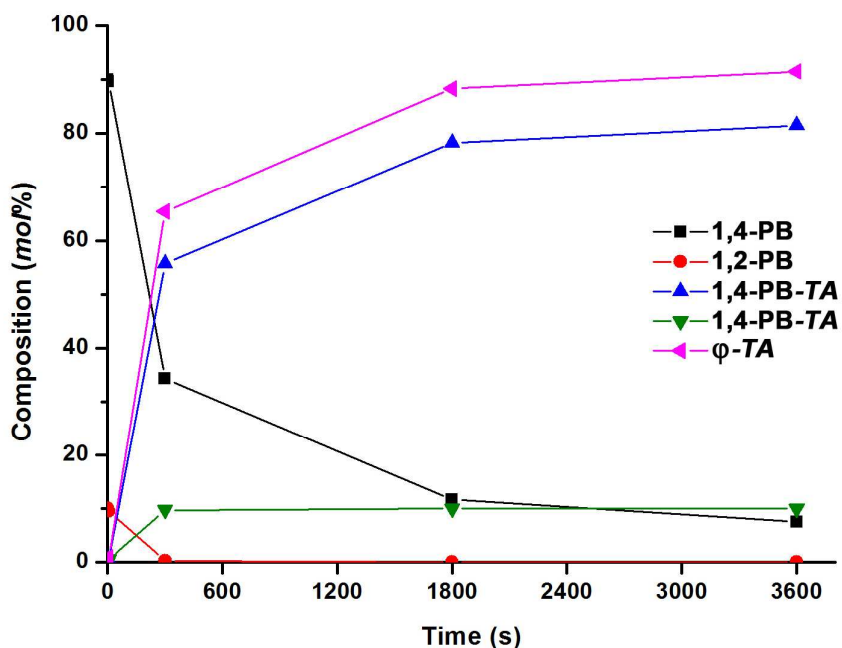


Figure S2. Plot of TAA addition to SBS activated with BZP and irradiation with UV light (entry 4, Table 1 and S2).

3. NMR CHARACTERIZATION.

3.1. ^{13}C NMR spectrum of **PB-TA**.

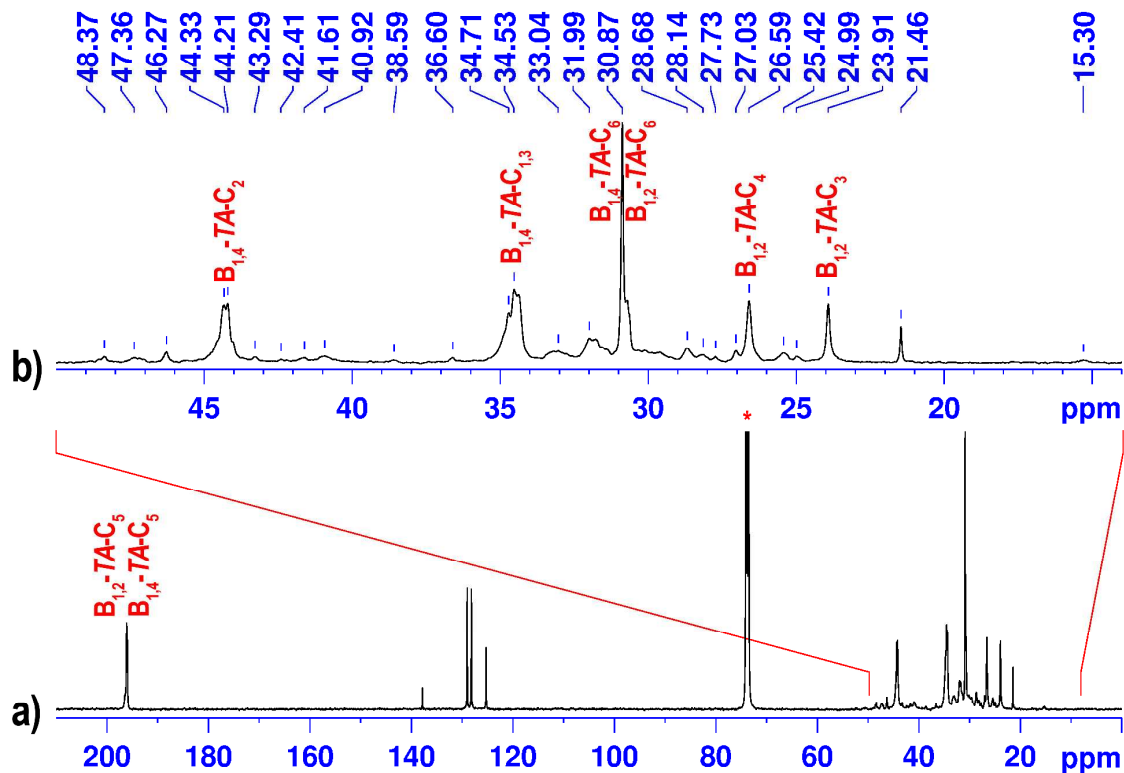


Figure S3. a) ^{13}C NMR spectrum (TCDE, 25°C) of **PB-TA** (entry 3, Table 1); b) magnification of the 50-14 ppm spectral region.

3.2. DEPT135- ^1H -HETCOR spectrum of **PB-TA.**

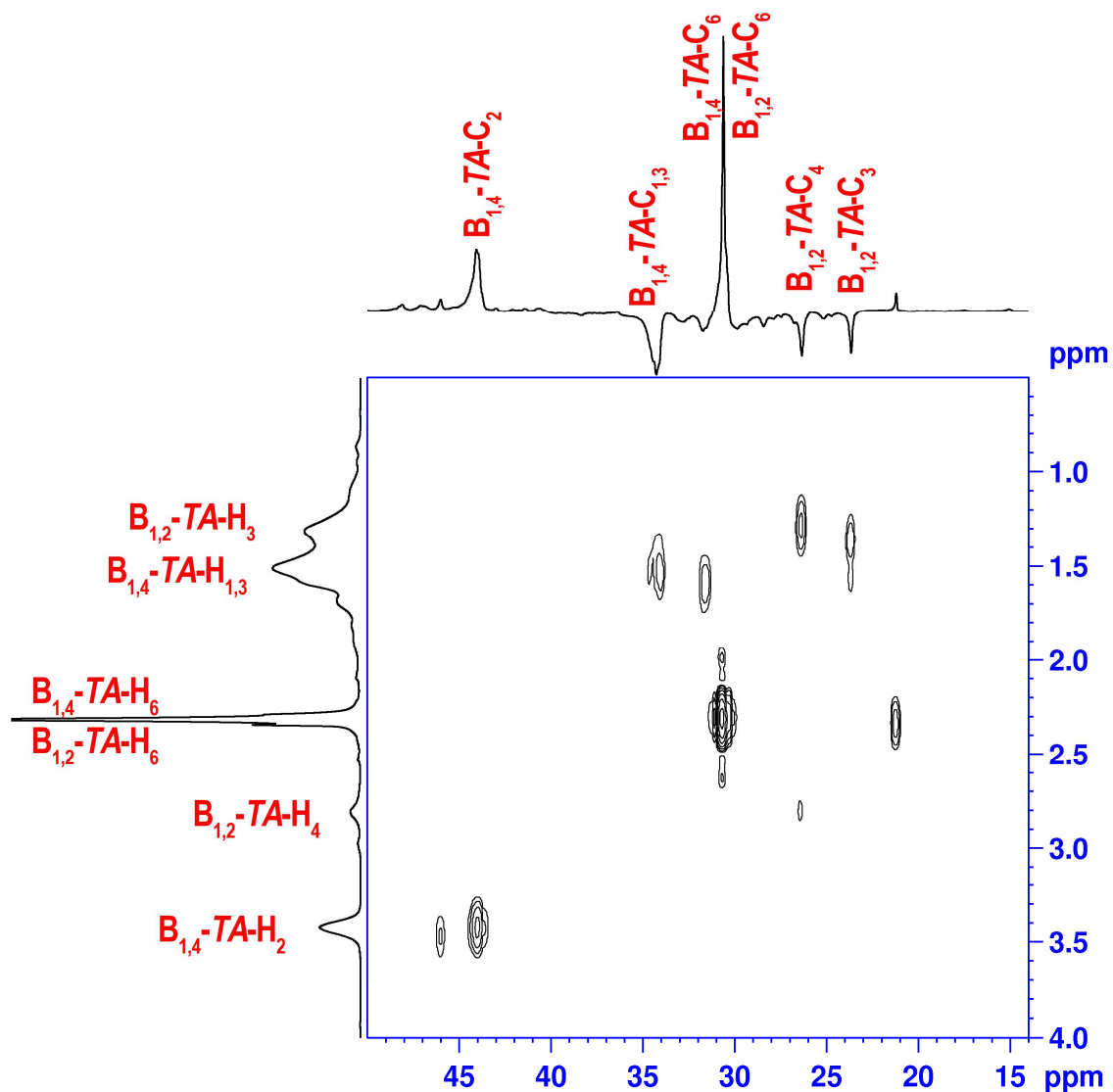


Figure S4. $^1\text{H}/^{13}\text{C}$ -DEPT135 HETCOR spectrum (300 MHz, TCDE, 25°C) of **PB-TA** (entry 3, Table 1).

3.3. ^1H - ^{13}C HSQC spectrum of **PB-TA**.

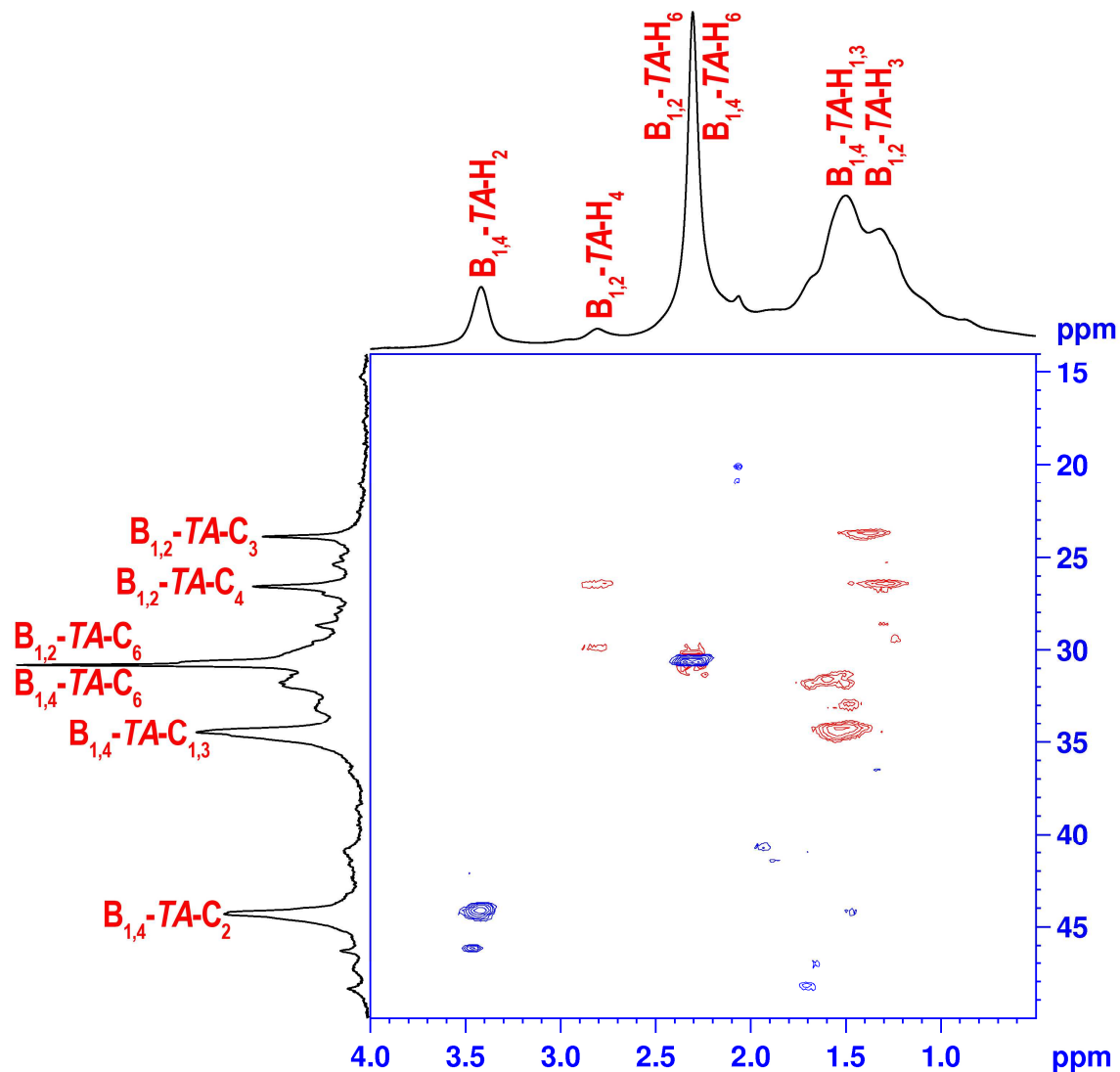


Figure S5. ^1H - ^{13}C HSQC spectrum (400 MHz, TCDE; 25°C) of **PB-TA** (entry 3, Table 1); the correlation spots due to methyl and methine signals are in blue, methylene in red .

3.4. ^1H - ^1H DQF-COSY spectrum of PB-*TA*.

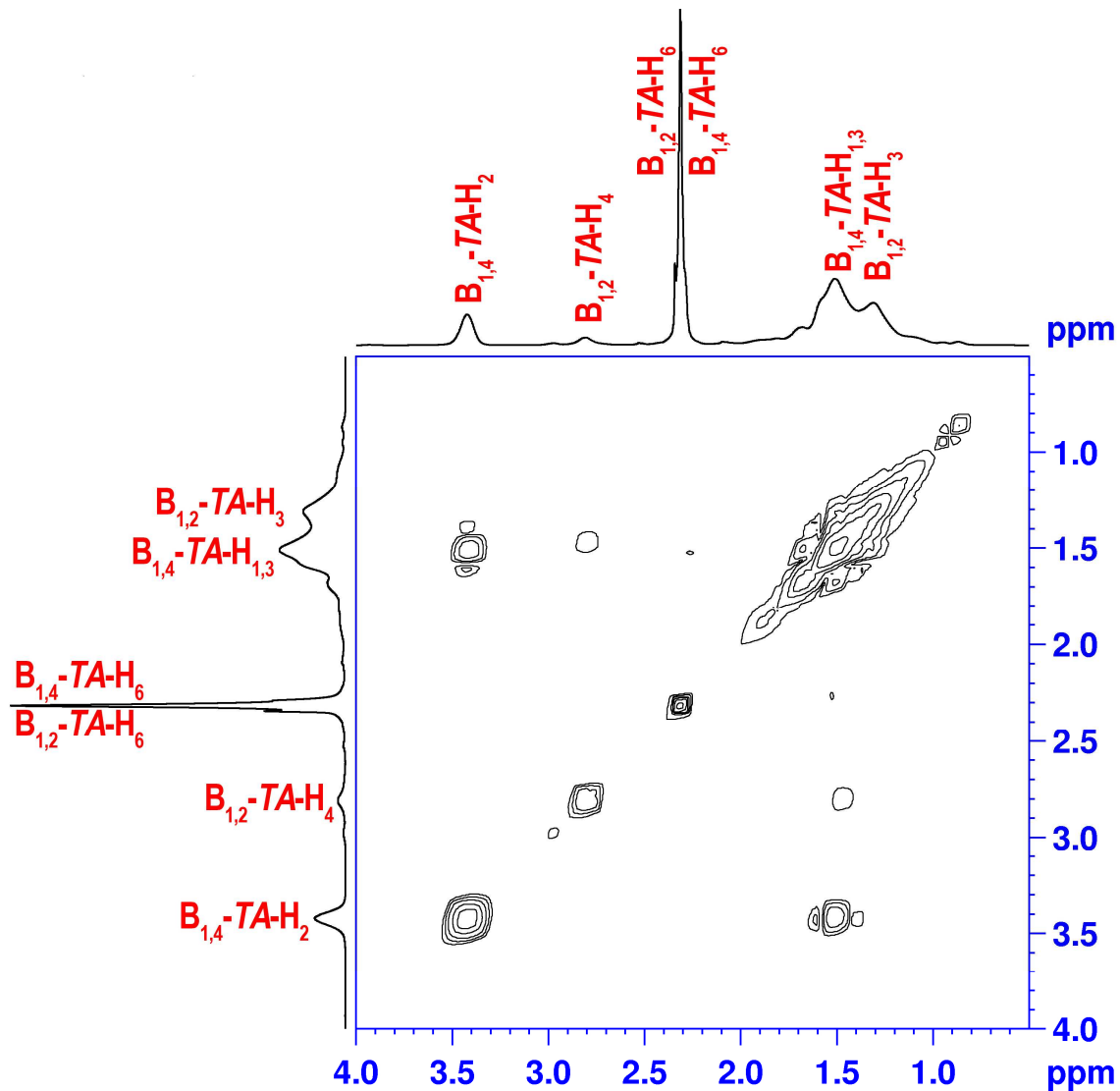


Figure S6. ^1H - ^1H DQF-COSY spectrum (250 MHz, TCDE, 25°C) of PB-*TA* (entry 3, Table 1).

3.5. ^{13}C NMR spectrum of PB-SA.

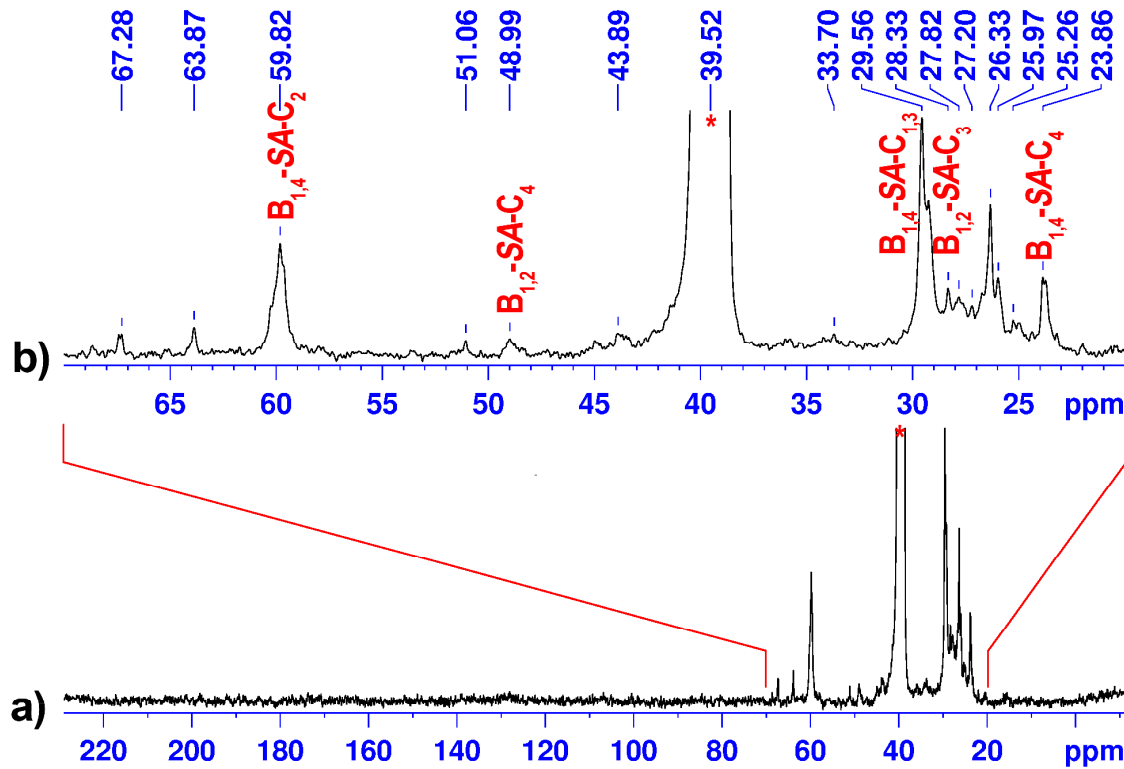


Figure S7. a) ^{13}C NMR spectrum (300 MHz, $^*\text{DMSO-d}_6$, 90°C) of PB-SA (entry 8, Table 3); b) magnification of the 70–20 ppm spectral region

3.6. DEPT135- ^1H HETCOR spectrum of PB-SA.

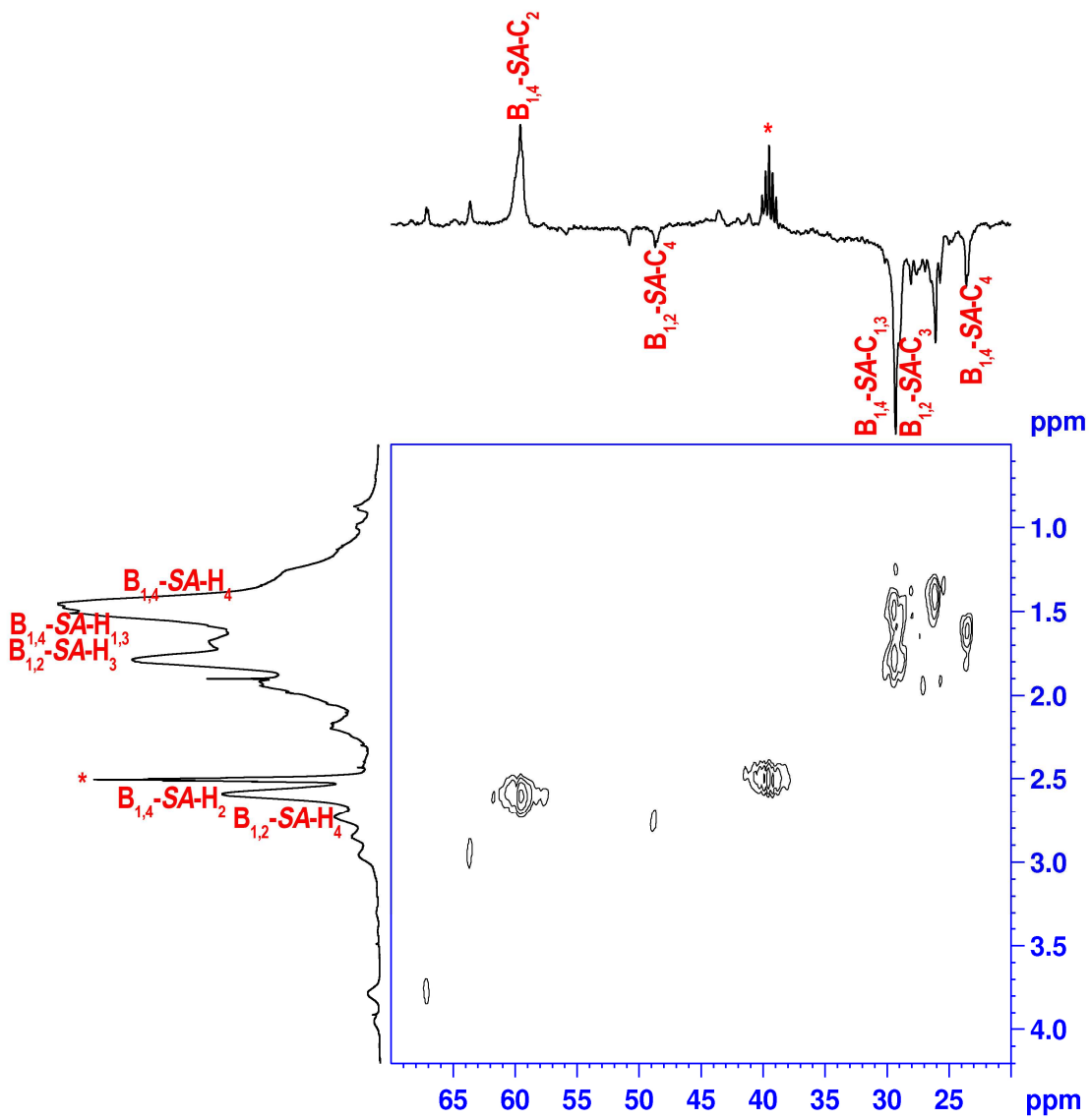


Figure S8. ^1H - ^{13}C -DEPT135 HETCOR spectrum (300 MHz, * DMSO-d_6 , 90°C) of **PB-SA** (entry 8, Table 3).

3.7. ^1H - ^1H DQF-COSY spectrum of PB-SA.

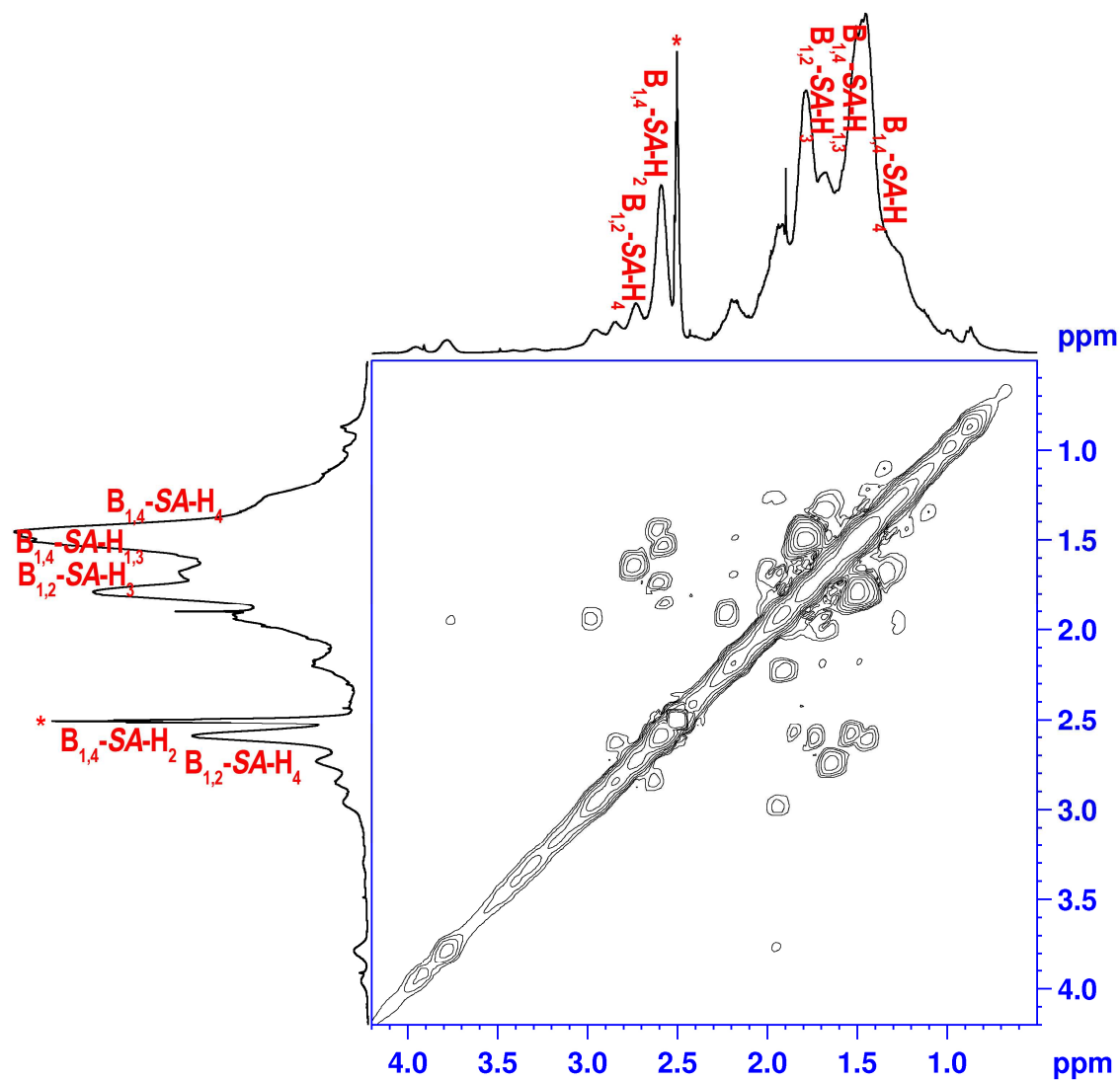


Figure S9. ^1H - ^1H DQF-COSY spectrum (250 MHZ, *DMSO-d₆, 90°C) of PB-SA (entry 8, Table 3).

3.8. ^1H NMR spectrum of S(B-TA)S.

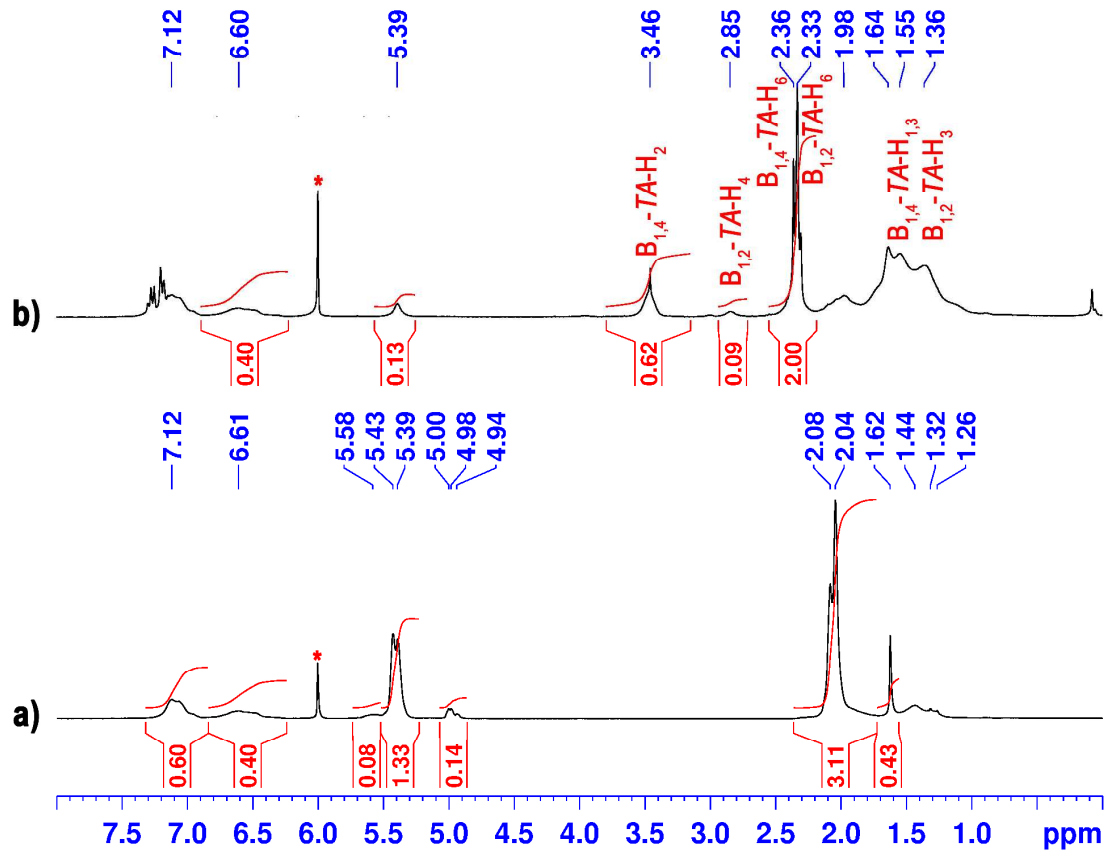


Figure S10. ^1H -NMR spectra (400 MHz, ^1H -TCDE, 25°C) of: a) SBS and b) S(B-TA)S (entry 4, Table 1). The characteristic signals of polystyrene were not labelled for simplicity.

3.9. ^{13}C NMR spectrum of S(B-TA)S.

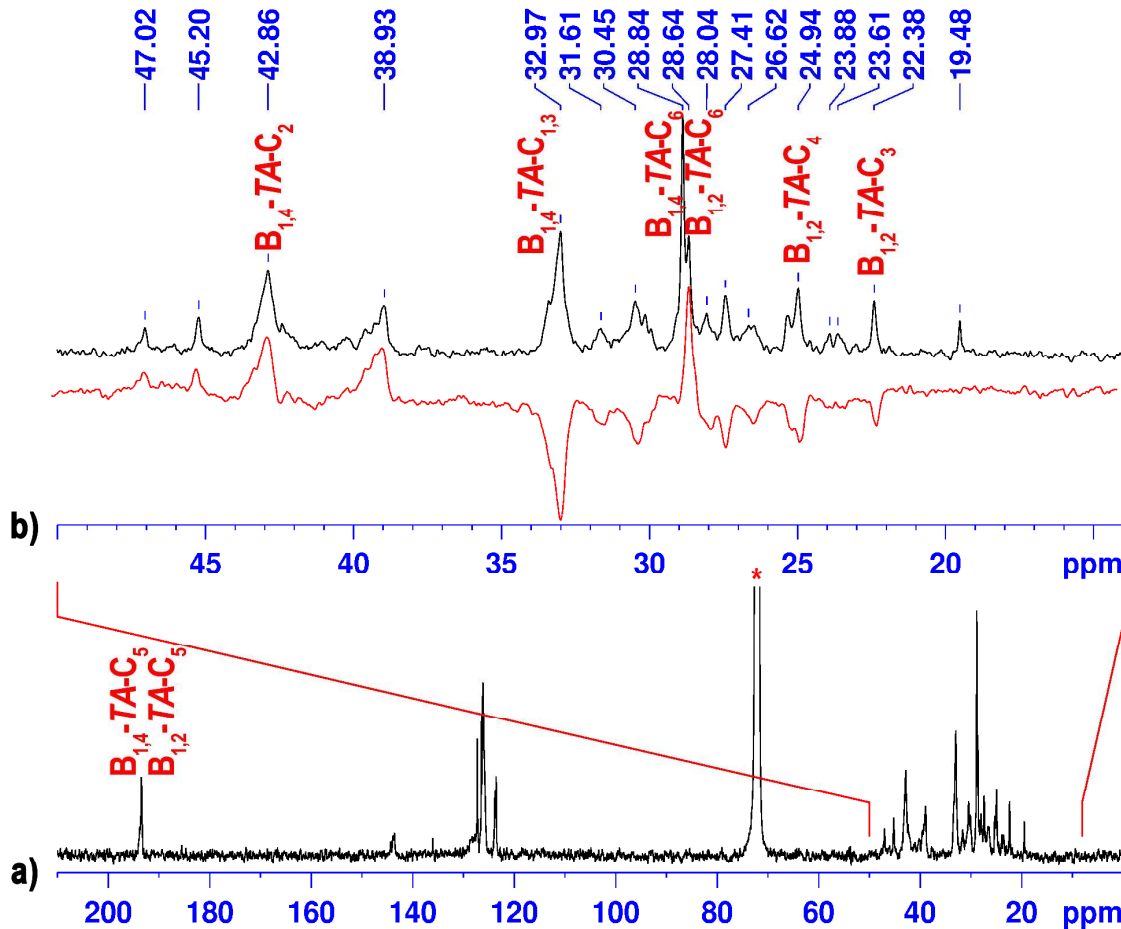


Figure S11. a) ^{13}C -NMR spectrum ($^{\star}\text{TCDE}$, 25°C) of **S(B-TA)S** (entry 7, Table 1); b)magnification of the region 50-14 ppm (black curve) and of the DEPT135 spectrum (red curve). The characteristic signals of polystyrene were not labelled for simplicity.

3.10. ^1H NMR spectrum of S(B-SA)S.

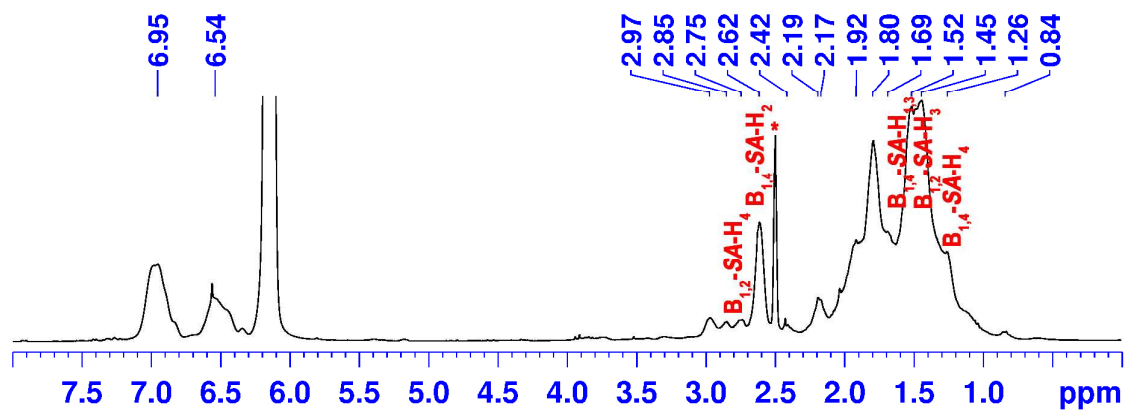


Figure S12. ^1H NMR spectrum (300 MHz, $^*\text{DMSO-d}_6$ /TCDE, $v/v = 3:1$, 90°C) of S(B-TA)S (entry 9, Table 3). The characteristic signals of polystyrene were not labelled for simplicity.

3.11. ^{13}C NMR spectrum of S(B-SA)S.

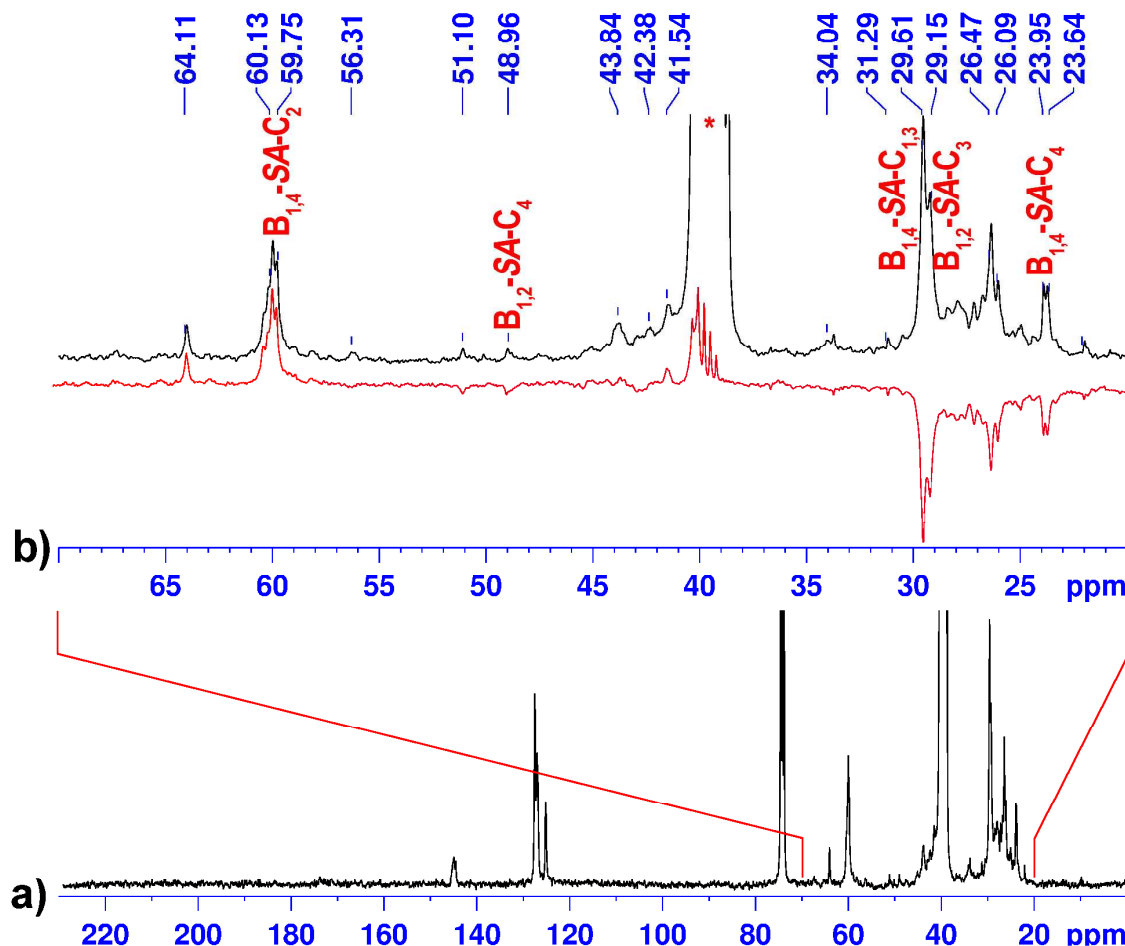


Figure S13. a) ^{13}C NMR spectrum (DMSO- d_6 /TCDE, $v/v = 3:1$, 90°C) of S(B-SA)S (entry 9, Table 3); b) magnification of the region 50-14 ppm (black curve) and of the DEPT135 spectrum (red curve). The characteristic signals of polystyrene were not labelled for simplicity.

4. FTIR CHARACTERIZATION.

4.1. FTIR spectra of SBS, S(B-TA) and S(B-SA)S.

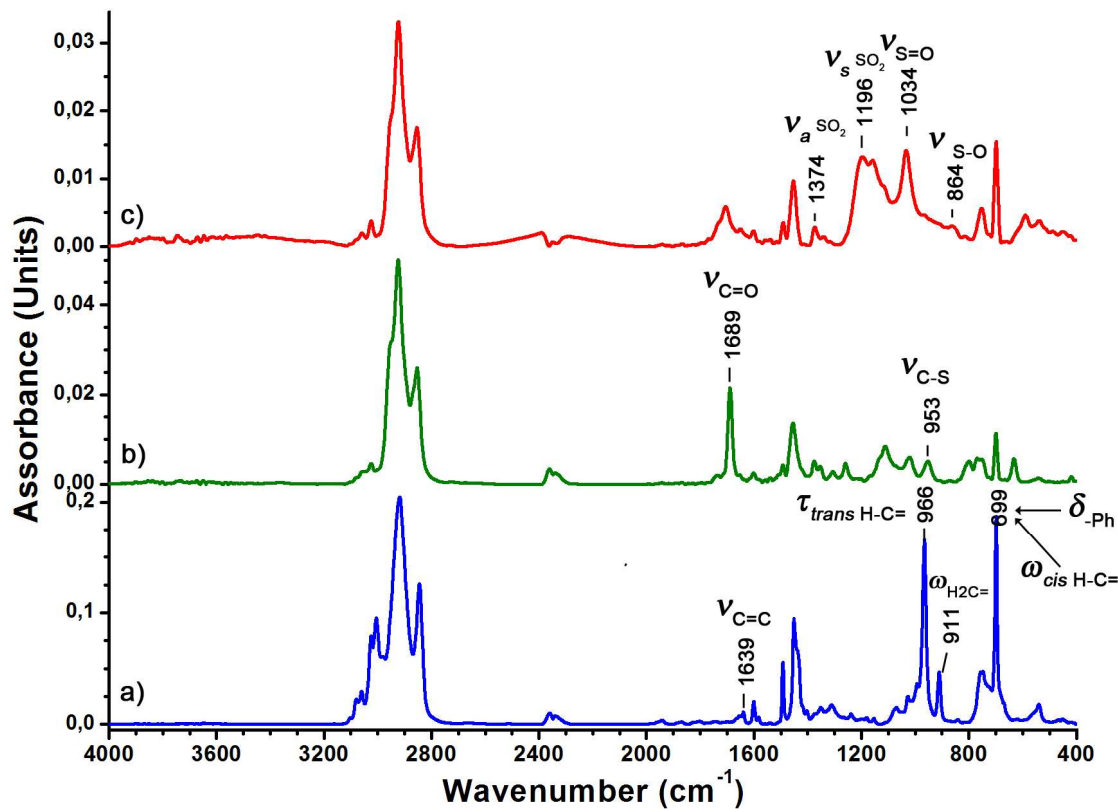


Figure S14. FTIR spectra of: a) SBS; b) S(B-TA)S (entry 7, Table 1); c) S(B-SA)S (entry 9, Table 3).

4.2. FTIR assignments.

Table S3. Main FTIR vibration assignments.

Polymer	Moiety	Mode	Intensity	Wavelength (cm ⁻¹)
PB	C=C	stretching	medium	1640
	<i>vinyl</i> H ₂ C=	deformation	strong	912
	<i>cis</i> H-C=	deformation	strong	737
PB-TA	C=O	stretching	strong	1689
	C-S	stretching	medium	953
PB-SA	SO ₂	antisymmetric stretching	medium	1334
	SO ₂	symmetric stretching	strong	1180
	S=O	stretching	strong	1036
	S-O	stretching	medium	861
SBS	C=C	stretching	medium	1639
	<i>vinyl</i> H ₂ C=	deformation	strong	911
	<i>trans</i> H-C=	deformation	strong	966
	<i>cis</i> H-C=	deformation	strong	699
	C-Ph	bending	strong	699
S(B-TA)S	C=O	stretching	strong	1689
	C-S	stretching	medium	953
	C-Ph	bending	strong	699
S(B-SA)S	SO ₂	antisymmetric stretching	medium	1374
	SO ₂	symmetric stretching	strong	1196
	S=O	stretching	strong	1034
	S-O	stretching	medium	864
	C-Ph	bending	strong	699

5.TGA and TGA-IR CHARACTERIZATION.

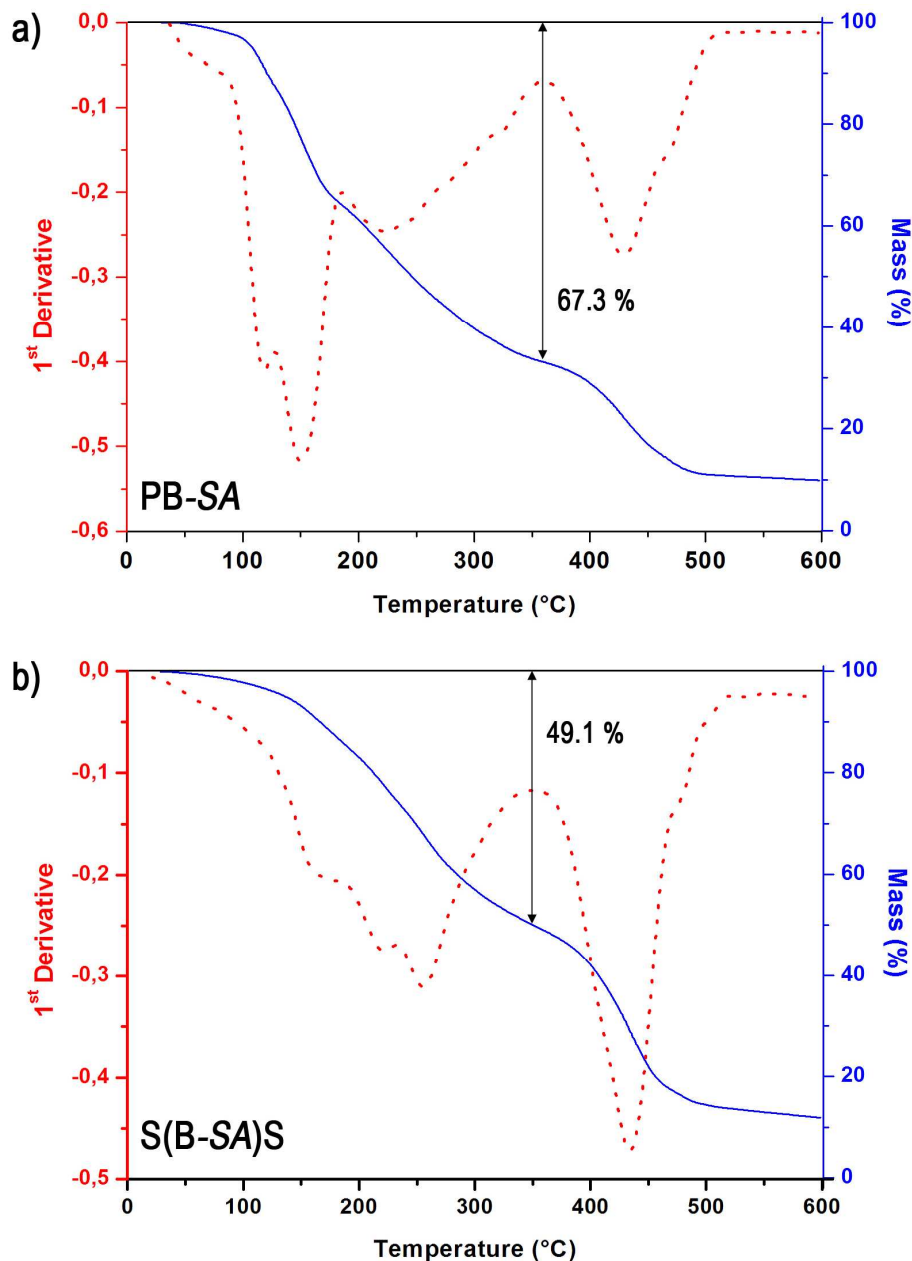


Figure S15. TGA traces (blue) and 1^{st} derivative curves (red) showing the weight loss due to desulfonation and decomposition of: a) **PB-SA**; b) **S(B-SA)S**.

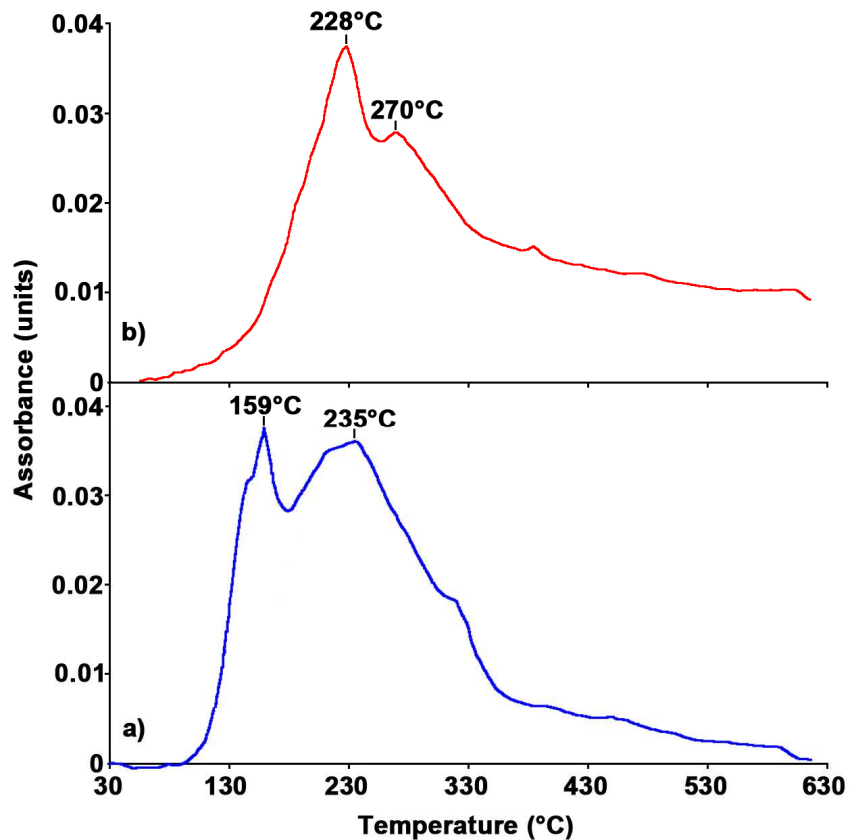


Figure S16. Plot of SO_2 thermal evolution by TGA–IR (signals at 1345 cm^{-1}) from: a) PB–SA (entry 8, Table 3); b) S(B–SA)S (entry 9, Table 3).

6. AFM Analysis of S(B-SA)S.

6.1. Dimension Distribution Analysis of PS domains in thin films of S(B-SA)S.

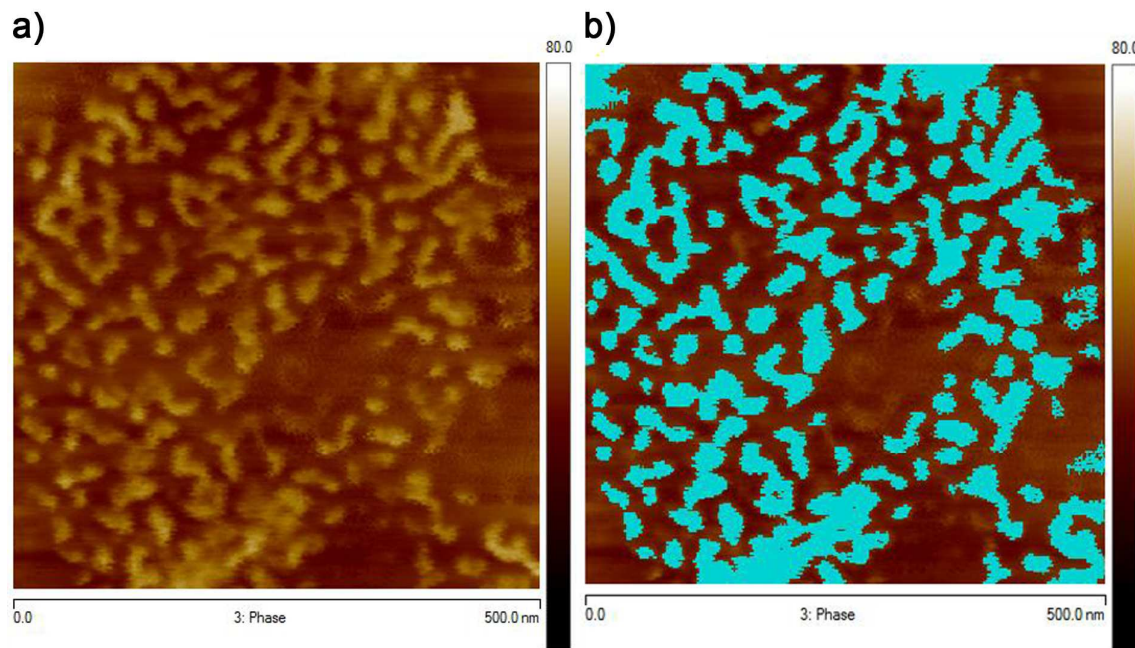


Figure S17. TM-AFM phase images of S(B-SA)S (entry 9, Table 3; scan size = 500 nm, z-scale = 80 deg): a) as acquired; b) with PS domains highlighted for the dimension distribution analysis performed with Nanoscope Analysis v1.40 r2sr1 software from Bruker.

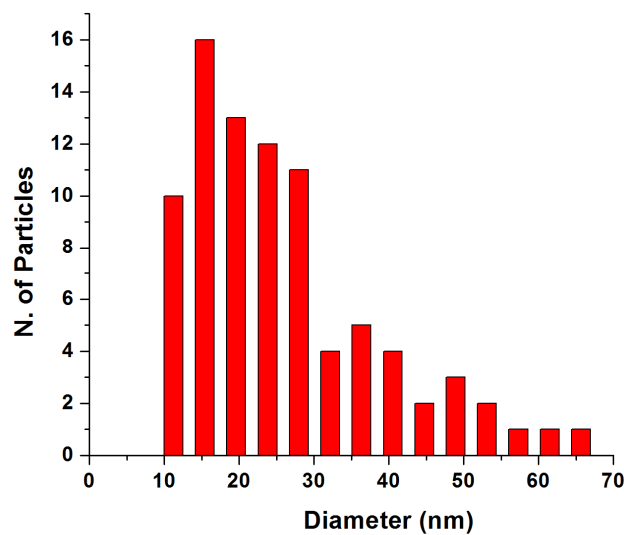


Figure S18. Dimension distribution analysis of PS domains of Figure S17 b.

6.2. TUNA-AFM characterization of thin films of S(B-SA)S.

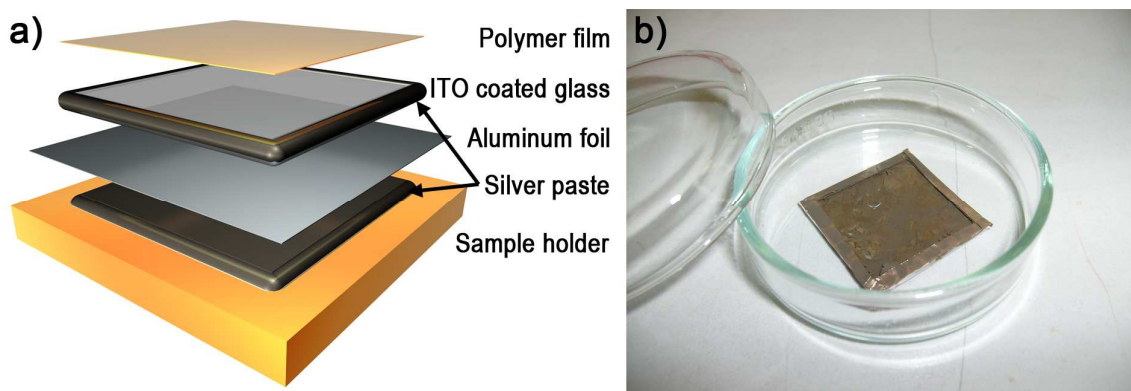


Figure S19. a) Schematic representation of the conductive support for TUNA-AFM measurements. b) The device.

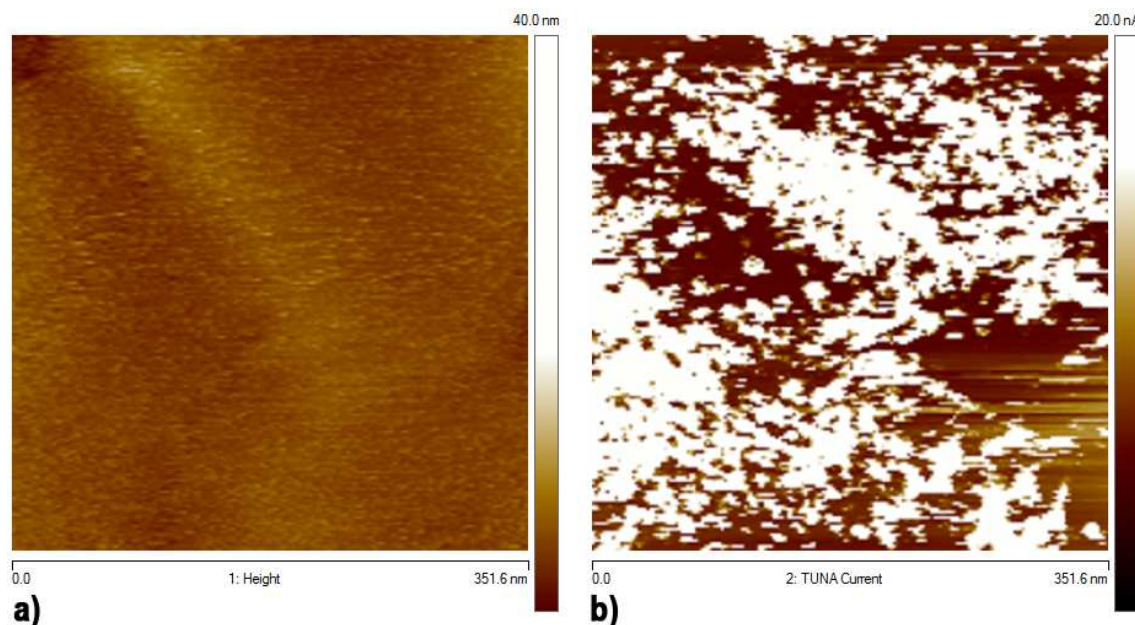


Figure S20. 2D TUNA-AFM micrographs of S(B-SA)S (entry 9, Table 3) corresponding to the image in Figure 5 c: a) height image (scan size = 350 nm, z-scale = 40 nm); b) TUNA Current (scan size = 350 nm, z-scale = 20 nA).